AD-A242 009

NCEL
## Contract Report

Three-Dimensional and Plane Stress Constitutive Models and Algorithms for Reinforced Concrete Plate and Shell Structures Incorporating Anisotropic Damage Mechanisms and Viscous Regularization Effects

ABSTRACT Three-dimensional and plane stress constitutive theories and algorithms are presented for reinforced concrete plate and shell structures. Anisotropic damage mechanisms are incorporated for representing the sundry failure modes exhibited by reinforced concrete subjected to intense dynamic loadings. Viscous regularization is employed for the representation of rate-dependent effects entailed by high rates of loading, and to mitigate numerical difficulties, such as spurious mesh sensitivity, brought about by strain softening behavior. Multiple failure surface theories and algorithms are also presented so that the present work can be applied to popular models appearing in the literature (e.g., the cap model).

91-14327
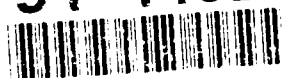
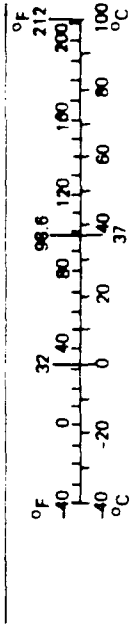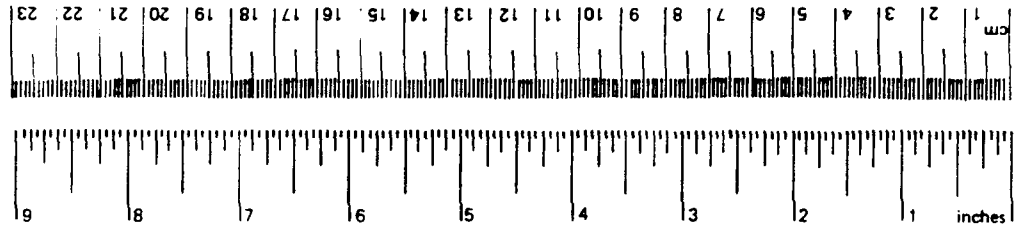**NAVAL CIVIL ENGINEERING LABORATORY PORT HUENEME CALIFORNIA 93043**

91 1υ ≈υ 114

METRIC CONVERSION FACTORS

Approximate Conversions to Metric Measures

Symbol	When You Know	Multiply by	To Find	Symbol
		LENGTH		
in	inches	*2.5	centimeters	cm
ft	feet	30	centimeters	cm
yd	yards	0.9	meters	m
mi	miles	1.6	kilometers	km
		AREA		
in^2	square inches	6.5	square centimeters	cm^2
ft^2	square feet	0.09	square meters	m^2
yd^2	square yards	0.8	square meters	m^2
mi^2	square miles	2.6	square kilometers	km^2
	acres	0.4	hectares	ha
		MASS (weight)		
oz	ounces	28	grams	g
lb	pounds	0.45	kilograms	kg
	short tons (2,000 lb)	0.9	tonnes	t
		VOLUME		
tsp	teaspoons	5	milliliters	ml
Tbsp	tablespoons	15	milliliters	ml
fl oz	fluid ounces	30	milliliters	ml
c	cups	0.24	liters	l
pt	pints	0.47	liters	l
qt	quarts	0.95	liters	l
gal	gallons	3.8	liters	l
ft^3	cubic feet	0.03	cubic meters	m^3
yd^3	cubic yards	0.76	cubic meters	m^3
		TEMPERATURE (exact)		
°F	Fahrenheit temperature	5/9 (after subtracting 32)	Celsius temperature	°C

*1 in 2.54 (exactly). For other exact conversions and more detailed tables, see NBS Misc. Publ. 286, Units of Weights and Measures, Price $2 25, SD Catalog No C13 10 286.

Approximate Conversions from Metric Measures

Symbol	When You Know	Multiply by	To Find	Symbol
		LENGTH		
mm	millimeters	0.04	inches	in
cm	centimeters	0.4	inches	in
m	meters	3.3	feet	ft
m	meters	1.1	yards	yd
km	kilometers	0.6	miles	mi
		AREA		
cm^2	square centimeters	0.16	square inches	in^2
m^2	square meters	1.2	square yards	yd^2
km^2	square kilometers	0.4	square miles	mi^2
ha	hectares (10,000 m^2)	2.5	acres	
		MASS (weight)		
g	grams	0.035	ounces	oz
kg	kilograms	2.2	pounds	lb
t	tonnes (1,000 kg)	1.1	short tons	
		VOLUME		
ml	milliliters	0.03	fluid ounces	fl oz
l	liters	2.1	pints	pt
l	liters	1.06	quarts	qt
l	liters	0.26	gallons	gal
m^3	cubic meters	35	cubic feet	ft^3
m^3	cubic meters	1.3	cubic yards	yd^3
		TEMPERATURE (exact)		
°C	Celsius temperature	9/5 (then add 32)	Fahrenheit temperature	°F

REPORT DOCUMENTATION PAGE

Public reporting burden for this collection of information is estimated to average 1 hour per response, including the time for reviewing instructions, searching existing data sources, gathering and maintaining the data needed, and completing and reviewing the collection of information. Send comments regarding this burden estimate or any other aspect of this collection of information, including suggestions for reducing this burden, to Washington Headquarters Services, Directorate for Information and Reports, 1215 Jefferson Davis Highway, Suite 1204, Arlington, VA 22202-4302, and to the Office of Management and Budget, Paperwork Reduction Project (0704-0188), Washington, DC 20503.

1. AGENCY USE ONLY (Leave blank)	2. REPORT DATE August 1991	3. REPORT TYPE AND DATES COVERED Final; May 1988 through April 1990

4. TITLE AND SUBTITLE THREE-DIMENSIONAL AND PLANE STRESS CONSTITUTIVE MODELS AND ALGORITHMS FOR REINFORCED CONCRETE PLATE AND SHELL STRUCTURES INCORPORATING ANISOTROPIC DAMAGE MECHANISMS AND VISCOUS REGULARIZATION EFFECTS

5. FUNDING NUMBERS

C - N62583-88-P-0365

6. AUTHOR(S)

Thomas J.R. Hughes and Arthur Muller

7. PERFORMING ORGANIZATION NAME(S) AND ADDRESSE(S)

Thomas J. R. Hughes, Inc.
903 Cottrell Way
Stanford, CA 94305

8. PERFORMING ORGANIZATION REPORT NUMBER

CR 91.010

9. SPONSORING/MONITORING AGENCY NAME(S) AND ADDRESSE(S)

Office of the Chief of Naval Research
Arlington, VA 22217-5000

10. SPONSORING/MONITORING AGENCY REPORT NUMBER

11. SUPPLEMENTARY NOTES

12a. DISTRIBUTION/AVAILABILITY STATEMENT

Approved for public release; distribution is unlimited.

12b. DISTRIBUTION CODE

13. ABSTRACT (Maximum 200 words)

Three-dimensional and plane stress constitutive theories and algorithms are presented for reinforced concrete plate and shell structures. Anisotropic damage mechanisms are incorporated for representing the sundry failure modes exhibited by reinforced concrete subjected to intense dynamic loadings. Viscous regularization is employed for the representation of rate-dependent effects entailed by high rates of loading, and to mitigate numerical difficulties, such as spurious mesh sensitivity, brought about by strain softening behavior. Multiple failure surface theories and algorithms are also presented so that the present work can be applied to popular models appearing in the literature (e.g., the cap model).

14. SUBJECT TERMS

Reinforced concrete plate, shell structures, anisotropic damage, dynamic loadings, viscous regularization, plane stress constitutive models

15. NUMBER OF PAGES
85

16. PRICE CODE

17. SECURITY CLASSIFICATION OF REPORT	18. SECURITY CLASSIFICATION OF THIS PAGE	19. SECURITY CLASSIFICATION OF ABSTRACT	20. LIMITATION OF ABSTRACT
Unclassified	Unclassified	Unclassified	UL

Contents

A-1

Chapter 1

Introduction

The analysis of reinforced concrete structures presents numerous challenges to the structural analyst. Essential prerequisites to performing effective calculations of reinforced concrete behavior include

1. Constitutive relations that accurately model the damage incurred by the concrete during crushing and cracking.

2. Robust theories and numerical implementations that can capture strain softening.

3. An efficient methodology to model reinforcement.

In previous studies, the senior author has investigated various aspects of developing computational methods for reinforced concrete plate and shell structures. In [22] continuum based plate and shell theories were introduced for finite element modeling which

permitted differing constitutive behavior at different laminae to facilitate representation of reinforcement through the thickness. In [11] a comprehensive study of constitutive models and stress-point integration algorithms was performed. Elastoplastic and viscoplastic theories were presented and isotropic damage mechanisms included. The principles upon which integration algorithms could be designed were thoroughly discussed in the context of the convex cutting plane method, a widely used procedure in optimization theory [14], and application was made to the cap model which has been used for modeling soils and concrete. In [9] the state-of-the-art in finite element modeling techniques for reinforced concrete plate and shell structures was assessed and suggestions for further research work were made. Several areas delineated as important in [9] have been pursued in this study, and elsewhere (e.g., L. R. Herrmann and colleagues are performing research on the bond-slip problem under NCEL support[5]). A summary of this report follows.

In Chapter 2 we consider constitutive models and algorithms for three-dimensional reinforced concrete behavior. We begin in Section 2.1 with a brief discussion of explicit and implicit methods for integrating constitutive models. The cutting plane algorithm described in [11] may be classified as an explicit procedure, which entails advantages in certain circumstances, and disadvantages in others. The most proment implicit method, namely, the closest point projection algorithm, is described in Section 2.1.1 within the framework of a general elastoplastic theory previously considered in [11]. This algorithm overcomes numerical stability limitations in the viscoplastic case, at the price of somewhat

2

more involved calculations during each iteration. Viscoplastic regularization has been proposed as a useful device for circumventing difficulties induced by *strain softening*, which occurs during concrete crushing and cracking. Consequently, the closest point projection algorithm may prove a useful technique in the development of algorithms for reinforced concrete structures subjected to severe loading environments.

In Section 2.2 we introduce a class of rate-independent anisotropic elastic damage models. Previously, we investigated a simple class of isotropic damage models [11], but the hypothesis of isotropy precludes adequate representation of, for example, cracking, which clearly induces anisotropy. The theories described herein, studied previously by Simo [20] in another context, assume that the elastic moduli are damage parameters and evolve according to a damage evolution law. The failure surface automatically induces an anisotropic damage mechanism. Likewise, the theory accomodates initially undamaged anisotropic elastic moduli, which are necessary for representing even the linear elastic response of reinforced concrete when viewed as a homogeneous continuum.

In Section 2.3 we present algorithms for the rate-independent anisotropic elastic damage model. Fully implicit algorithms are proposed in Section 2.3.1, but it is concluded that these methods entail calculations at the stress-point level which are too intensive for practical use in large-scale finite element analysis. Simpler explicit/implicit methods are introduced as alternatives in Section 2.3.2. The first of these algorithms freezes an

3

"update direction" at its initial value whereas in the second procedure the update direction is recomputed during each iteration in an explicit, multi-corrector fashion (see Hughes [10], Chapter 9, for related ideas in dynamics). The latter algorithm, referred to as the updated explicit/implicit algorithm, is viewed as simple enough for implementatation in large-scale finite element programs, while at the same time it "almost" attains full implicitness, a potential advantage with respect to accuracy and stability. As an example, we apply the theory in Section 2.4 to an elliptical failure surface in pressure-deviatoric stress space and specialize the updated explicit/implicit algorithm to this case.

A rate-dependent generalization of the damage model is presented in Section 2.5. The classical Perzyna idea of viscous regularization [16] is invoked in which the consistency parameter is replaced by a non-dimensional switching function, which turns on when the failure surface function is positive, divided by a relaxation-time parameter. A variant on the updated explicit/implicit algorithm is developed for the rate-dependent model in which a stable subincrementation strategy, as described in [11], is employed.

The damage constitutive models for three-dimensional analysis presented in Chapter 2 are useful for detailed modeling in regions of supports, haunches, and transition zones. They are also useful in the generation and qualification of plane stress analogs for plates and shells applicable to large-scale structural modeling.

Plane stress generalizations of the algorithms of Chapter 2 are presented in Chapter 3. The rate-independent and rate-dependent cases are presented in Sections 3.1 and 3.2, respectively. Use of these models in conjunction with plate and shell formulations is discussed in Section 3.3.

In previous research, attention has focused on the cap model for modeling concrete (see, e.g., [11]). The cap model falls within the framework of the general elastoplastic and viscoplastic theories considered in [11], except for the fact that it is a particular example of a so-called multiple yield surface theory. In the present framework of damage modeling, we are likewise concerned with multiple failure surfaces in analogy with multiple yield surfaces in elastoplasticity and viscoplasticity. For the cap model, we presented previously a concise algorithm for integrating the constitutive equation and efficiently handling the three branches of the yield surface. General approaches for handling multiple yield surfaces have been presented in [18,19]. Herein we adopt a more general point of view and in Chapter 4 develop multiple failure surface analogs of the single surface models and algorithms described in Chapters 2 and 3. The approach assumes "m" failure surfaces. Consequently, by taking $m = 3$, and specifying the failure surfaces to be those of the cap model, the approach reduces to cap-like anisotropic damages models. However, we believe the general approach has considerable potential in that different and more elaborate sets of failure surfaces will likely be more appropriate for modeling reinforced concrete including cracking, crushing, and bond slip.

5

The three-dimensional multiple failure surface, rate-independent anisotropic elastic damage model is presented in Section 4.1. The updated explicit/implicit algorithm for this case is developed in Section 4.1.1. Similar developments are carried out for the rate-dependent version in Sections 4.2 and 4.2.1. Plane stress analogs are examined in Sections 4.3 and 4.4. The rate-independent case is dealt with in Section 4.3 and the rate dependent case in Section 4.4. Conclusions are drawn in Chapter 5.

The present work allows for modeling reinforced concrete by way of point constitutive equations. The effect of concrete, reinforcement, and their interaction, is, in principle, representable by "homogenized", or distributed, constitutive relations. An approach of this kind represents an efficient alternative to those currently in use in which reinforcement and concrete are modeled separately, and bond-slip is generally ignored. What is required to make an approach of this kind a practical reality is characterization of the failure surfaces and hardening laws for reinforced concrete. All salient physical mechanisms, e.g., cracking, crushing, bond-slip, tension stiffening, shear retention, etc., are, in principle, subsumable within such an approach. On the other hand, the practical and specific realizations of the failure surfaces and hardening laws represents an essential but non-trivial endeavor. As a starting point for such an endeavor it seems useful to study the failure theory of fiber-reinforced composites. It is intuitevely clear that fiber-reinforced composites and reinforced concrete have many features in common. In particular, failure surfaces for fiber-reinforced composites have been studied extensively, e.g., one may men-

tion the well-known Tsai-Hill and Tsai-Wu criteria [12]. (An ellipsoid in stress space is a special case of Tsai-Wu, cf. Section 2.4). It is felt that a worthwhile avenue of approach for developing the detailed aspects of the types of models described herein begins with existing work in fiber-reinforced composites. One of course would need to identify the material parameters of the model selected. In principle, this could be done by testing "specimens" of actual fabricated reinforced concrete slabs; however, due to specimen size and the number of different tests required, this would appear impractical. On the other hand, assuming a constitutive model existed for *unreinforced* concrete that one had confidence in, and if a sufficiently accurate model of bond-slip behavior existed (see recent work of L. Herrmann and colleagues at U.C. Davis[5]), and employing standard elastoplastic modeling of steel rebars, then *computational* tests might be performed to determine the failure surface parameters for the "composite". These could subsequently be used to define the anisotropic damage reinforced concrete model.

Likewise, failure surfaces used for unreinforced concrete such as the well-known plane stress Kupfer surface [13] — see Figure 1.1 — and its three-dimensional generalizations could be used as failure surfaces for anisotropic damage models[1]. Constitutive equations of this kind are frequently combined with discrete truss-like or membrane-like equivalent rebar distributions in current capabilities (see, e.g., Cervera, Hinton, and colleagues [2,3] for representative approaches of this kind).

---

[1]The failure surface could likewise be the CAP yield surface used in previous studies.
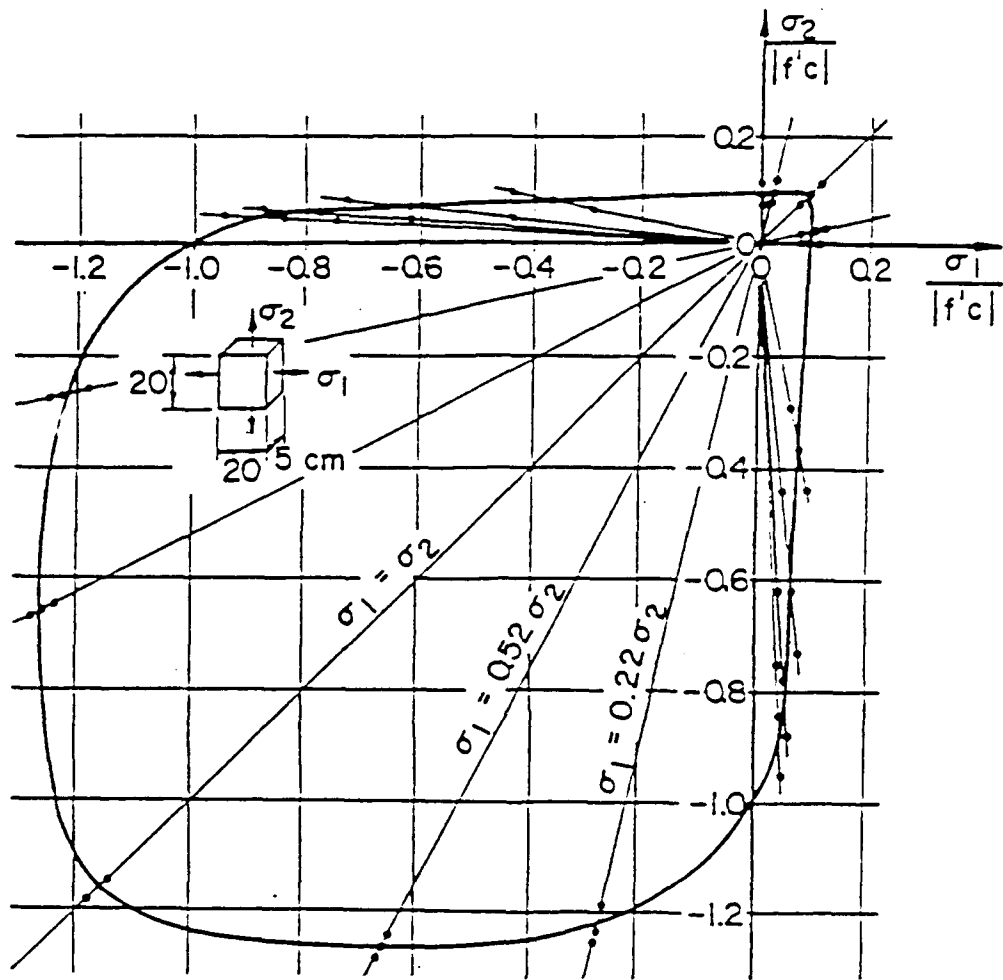
Figure 1.1: Bi-axial strength of concrete. f'_c stands for the uniaxial compressive strength.

An issue which needs to be emphasized when dealing with severely loaded reinforced concrete is strain softening. The theoretical and numerical sensitivities engendered by this phenomenon are still subjects of heated discussion in research circles. Essential insights into numerical difficulties (i.e., spurious mesh dependence) brought about by strain softening were presented in one of our previous studies [9]. Basically, two methodologies remain in use to deal with this problem. The first involves specifying key material parameters to depend upon finite element mesh length scales (e.g., the plastic modulus in an elastoplastic theory). This approach is throughly discussed in [9] and references cited therein. The second approach employs viscous regularization. Deficiencies noted for rate-independent elastoplastic models used to represent strain-softening are avoided by rate-dependent viscoplastic models obtained by a viscous regularization of the elastoplastic model. This approach has been advocated by several investigators. Valanis [23] has provided computational and theoretical results supporting this view. One of the main reasons we developed the rate-dependent versions of the anisotropic damage models in this report was to provide a practical means for dealing with strain softening behavior. Further research is, of course, still necessary on this topic. Nevertheless, within the spectrum of methods and algorithms presented herein, fundamental objections to specific classes of models (e.g., rate-independent elastoplastic models), may be overcome. In principle, the classical Perzyna viscous regularization employed herein also avoids the necessity of employing mesh-dependent material parameters as described in [9]. Likewise, the rate-

dependent mechanisms present allow for more faithful representation of material response to high rates of loading.

Throughout this report we focus our attention on small-deformation response. The generalization to finite deformations, necessary for modeling large translations and rotations associated with reinforced concrete plate and shell structural response to severe blast loadings, may be simply accomplished by procedures described in [8]. See also [18] for an update on approaches of this kind, and a description of their trials and tribulations. By way of these by now standard procedures, all that is developed herein may be immediately generalized to the finite-deformation case.

Chapter 2

Constitutive Models and Algorithms for Reinforced Concrete

2.1 Explicit and Implicit Methods

In a previous report (see [11]), general classes of inelastic constitutive equations were studied and their applicability to concrete was examined. It was pointed out that two general methodologies had emerged for the numerical integration of rate-independent inelastic constitutive equations: the *cutting plane algorithm* [14] and the *closest point projection algorithm* [18].

The cutting plane algorithm was discussed in detail in [11]. It avoids the evaluation of gradients and Hessians, and thus is computationally simpler than the closest point projection algorithm and therefore should be utilized whenever possible. However, severe limitations exist when a *viscous regularization* is employed: the cutting plane algorithm is

explicit and numerical stability conditions may engender excessively small subincremental time steps (see [11]). On the other hand, the closest point projection algorithm is *implicit* and unconditionally stable. Consequently, it offers a potentially superior alternative to the cutting plane algorithm when viscous effects are present in the constitutive theory. However, the closest point projection algorithm is more computationally intensive than the cutting plane algorithm per iteration, and thus this also needs to be weighed in any comparison.

The closest point projection algorithm will be illustrated below for a general class of rate-independent elastoplastic materials.

2.1.1 Closest Point Projection Algorithm

The following notations are employed:

k	Iteration counter
σ	Cauchy or true stress
ϵ	Total strain
ϵ^{pl}	Plastic strain
Ψ	Elastic strain energy density function
f	Yield function
$\mathbf{q}$	Strain-like internal hardening parameters
λ	Consistency parameter
$\mathbf{h}$	Function defining the direction of $\dot{\mathbf{q}}$
$\mathbf{r}$	Function defining the direction of $\dot{\epsilon}^{\mathrm{pl}}$
$\mathbf{c}$	Hessian of the elastic strain energy density function
$\mathbf{R}$	Residual vector in the Newton iteration
$\mathbf{A}$	Tangent matrix in the Newton iteration
$\mathbf{I}$	Identity tensor
TOL_1	Tolerance for feasible stress region
TOL_2	Tolerance for nonlinear residual

Partial derivatives are written in the following short-hand notation:

$$\partial_{\sigma} f = \frac{\partial f}{\partial \sigma} \tag{2.1}$$

$$\partial_{\mathbf{q}} f = \frac{\partial f}{\partial \mathbf{q}} \tag{2.2}$$

$$\partial^2_{\sigma \mathbf{q}} f = \frac{\partial^2 f}{\partial \sigma \partial \mathbf{q}}, \text{etc.} \tag{2.3}$$

13

The theory employed has been presented in [11]. For completeness we recall it here. For further details, the reader is urged to consult [11].

Box 1. *A small-deformation rate-independent elastoplastic constitutive theory.*

Constitutive equation:

$$\boldsymbol{\sigma} = \partial_\epsilon \Psi \left(\epsilon - \epsilon^{\mathrm{pl}} \right) \tag{2.4}$$

Hardening law:

$$\dot{\mathbf{q}} = \dot{\lambda} \mathbf{h}(\boldsymbol{\sigma}, \mathbf{q}) \tag{2.5}$$

Flow rule:

$$\dot{\epsilon}^{\mathrm{pl}} = \dot{\lambda} \mathbf{r}(\boldsymbol{\sigma}, \mathbf{q}) \tag{2.6}$$

Loading/unloading conditions:

$$\dot{\lambda} \geq 0 \tag{2.7}$$

$$f(\boldsymbol{\sigma}, \mathbf{q}) \leq 0 \tag{2.8}$$

$$\dot{\lambda} f(\boldsymbol{\sigma}, \mathbf{q}) = 0 \tag{2.9}$$

Remarks:

1. Note that the elastic constitutive law may be *nonlinear* and the flow rule may be nonassociative. In the associative case

$$\mathbf{r} = \partial_{\boldsymbol{\sigma}} f \tag{2.10}$$

2. The loading/unloading conditions are written concisely in the so-called Kuhn-Tucker form of optimization theory.

3. The consistency condition yields the following expression for $\dot{\lambda}$:

$$\dot{\lambda} = \frac{\partial_{\boldsymbol{\sigma}} f \cdot \mathbf{c}\dot{\epsilon}}{\left(\partial_{\boldsymbol{\sigma}} f \cdot \mathbf{c}\mathbf{r} - \partial_{\mathbf{q}} f \cdot \mathbf{h}\right)} \tag{2.11}$$

The closest point projection algorithm is given by Algorithm 1[17]:

Algorithm 1. *Closest point projection algorithm for the small-deformation rate-independent elastoplastic theory of Box 1.*

Step 1. Initialize:

$$k = 0 \tag{2.12}$$

$$\epsilon_{n+1}^{\mathrm{pl}(0)} = \epsilon_n^{\mathrm{pl}} \tag{2.13}$$

$$\mathbf{q}_{n+1}^{(0)} = \mathbf{q}_n \tag{2.14}$$

$$\delta\lambda_{n+1}^{(0)} = 0 \tag{2.15}$$

Step 2. Compute stress, yield function and flow rule and hardening law residuals:

$$\boldsymbol{\sigma}_{n+1}^{(k)} = \partial_\epsilon \Psi \left(\epsilon_{n+1} - \epsilon_{n+1}^{\mathrm{pl}(k)} \right) \tag{2.16}$$

$$f_{n+1}^{(k)} = f \left(\boldsymbol{\sigma}_{n+1}^{(k)}, \mathbf{q}_{n+1}^{(k)} \right) \tag{2.17}$$

$$\mathbf{R}_{n+1}^{(k)} = \left\{ \begin{array}{c} -\epsilon_{n+1}^{\mathrm{pl}(k)} + \epsilon_n^{\mathrm{pl}} \\ -\mathbf{q}_{n+1}^{(k)} + \mathbf{q}_n \end{array} \right\} + \delta\lambda_{n+1}^{(k)} \left\{ \begin{array}{c} \mathbf{r}_{n+1}^{(k)} \\ \mathbf{h}_{n+1}^{(k)} \end{array} \right\} \tag{2.18}$$

If $((k = 0$ and $f_{n+1}^{(k)} \leq \mathrm{TOL}_1)$ or $(|f_{n+1}^{(k)}| \leq \mathrm{TOL}_1$ and $\|\mathbf{R}_{n+1}^{(k)}\| \leq \mathrm{TOL}_2))$ then

$$\epsilon_{n+1}^{\mathrm{pl}} = \epsilon_{n+1}^{\mathrm{pl}(k)} \tag{2.19}$$

$$\mathbf{q}_{n+1} = \mathbf{q}_{n+1}^{(k)} \tag{2.20}$$

return

endif

Step 3. Compute elastic moduli and consistent tangent moduli:

$$\mathbf{c}_{n+1}^{(k)} = \partial_{\epsilon\epsilon}^2 \Psi \left(\epsilon_{n+1} - \epsilon_{n+1}^{\mathrm{pl}(k)} \right) \tag{2.21}$$

$$\mathbf{A}_{n+1}^{(k)} = \left[\begin{array}{cc} \left[\left(\mathbf{c}_{n+1}^{(k)}\right)^{-1} + \delta\lambda_{n+1}^{(k)} \partial_\sigma \mathbf{r}_{n+1}^{(k)} \right] & \delta\lambda_{n+1}^{(k)} \partial_\mathbf{q} \mathbf{r}_{n+1}^{(k)} \\ \delta\lambda_{n+1}^{(k)} \partial_\sigma \mathbf{h}_{n+1}^{(k)} & -\mathbf{I} + \delta\lambda_{n+1}^{(k)} \partial_\mathbf{q} \mathbf{h}_{n+1}^{(k)} \end{array} \right]^{-1} \tag{2.22}$$

Step 4. Calculate increment of consistency parameter:

$$\Delta\lambda_{n+1}^{(k)} = \frac{f_{n+1}^{(k)} - \left[\begin{array}{cc} \partial_\sigma f_{n+1}^{(k)} & \partial_\mathbf{q} f_{n+1}^{(k)} \end{array} \right] \mathbf{A}_{n+1}^{(k)} \mathbf{R}_{n+1}^{(k)}}{\left[\begin{array}{cc} \partial_\sigma f_{n+1}^{(k)} & \partial_\mathbf{q} f_{n+1}^{(k)} \end{array} \right] \mathbf{A}_{n+1}^{(k)} \left\{ \begin{array}{c} \mathbf{r}_{n+1}^{(k)} \\ \mathbf{h}_{n+1}^{(k)} \end{array} \right\}} \tag{2.23}$$

Step 5. Calculate incremental plastic strains and internal variables:

$$\left\{ \begin{array}{c} \Delta\epsilon^{\mathrm{pl}(k)}_{n+1} \\ \Delta\mathbf{q}^{(k)}_{n+1} \end{array} \right\} = \left[\begin{array}{cc} \left(\mathbf{c}^{(k)}_{n+1}\right)^{-1} & \mathbf{0} \\ \mathbf{0} & -\mathbf{I} \end{array} \right] \mathbf{A}^{(k)}_{n+1} \left[\mathbf{R}^{(k)}_{n+1} + \Delta\lambda_{n+1} \left\{ \begin{array}{c} \mathbf{r}^{(k)}_{n+1} \\ \mathbf{h}^{(k)}_{n+1} \end{array} \right\} \right] \quad (2.24)$$

Step 6. Update plastic strain, hardening and consistency parameters:

$$\epsilon^{\mathrm{pl}(k+1)}_{n+1} = \epsilon^{\mathrm{pl}(k)}_{n+1} + \Delta\epsilon^{\mathrm{pl}(k)}_{n+1} \quad (2.25)$$

$$\mathbf{q}^{(k+1)}_{n+1} = \mathbf{q}^{(k)}_{n+1} + \Delta\mathbf{q}^{(k)}_{n+1} \quad (2.26)$$

$$\delta\lambda^{(k+1)}_{n+1} = \delta\lambda^{(k)}_{n+1} + \Delta\lambda^{(k)}_{n+1} \quad (2.27)$$

Set $k = k + 1$ and go to Step 2.

Remarks:

1. The above algorithm is conceptually simple: the rate equations are integrated via an Euler backward-difference scheme and the resulting (nonlinear) equations are then solved with Newton's method. A sketch of the derivation is provided for the interested reader:

Backward difference formulas:

$$\epsilon^{\mathrm{pl}}_{n+1} = \epsilon^{\mathrm{pl}}_n + \delta\lambda_{n+1}\mathbf{r}_{n+1} \quad (2.28)$$

$$\mathbf{q}_{n+1} = \mathbf{q}_n + \delta\lambda_{n+1}\mathbf{h}_{n+1} \quad (2.29)$$

$$\delta\lambda_{n+1} = \lambda_{n+1} - \lambda_n \quad (2.30)$$

17

Newton's method:

Linearization is performed about the kth iterative approximation to state $n+1$. The notation "Δ" is used to denote the difference between consecutive iterates, e.g.,

$$\Delta \lambda_{n+1}^{(k)} = \lambda_{n+1}^{(k+1)} - \lambda_{n+1}^{(k)} \tag{2.31}$$

This should be contrasted with the use of "δ", i.e.,

$$\delta \lambda_{n+1}^{(k)} = \lambda_{n+1}^{(k)} - \lambda_n \tag{2.32}$$

We need to evaluate the backward difference formulas at iterate $k+1$ and linearize about iterate k, viz.

$$\epsilon_{n+1}^{\text{pl}(k+1)} = \epsilon_n^{\text{pl}} + \delta\lambda_{n+1}^{(k+1)} \mathbf{r}_{n+1}^{(k+1)} \tag{2.33}$$

$$\mathbf{q}_{n+1}^{(k+1)} = \mathbf{q}_n + \delta\lambda_{n+1}^{(k+1)} \mathbf{h}_{n+1}^{(k+1)} \tag{2.34}$$

$$\begin{aligned}
\epsilon_{n+1}^{\text{pl}(k)} + \Delta\epsilon_{n+1}^{\text{pl}(k)} &\approx \epsilon_n^{\text{pl}} + \Delta\lambda_{n+1}^{(k)}\mathbf{r}_{n+1}^{(k)} + \delta\lambda_{n+1}^{(k)}\left(\mathbf{r}_{n+1}^{(k)} + \Delta\mathbf{r}_{n+1}^{(k)}\right) \\
&= \epsilon_n^{\text{pl}} + \Delta\lambda_{n+1}^{(k)}\mathbf{r}_{n+1}^{(k)} + \\
&\quad \delta\lambda_{n+1}^{(k)}\left(\mathbf{r}_{n+1}^{(k)} + \partial_{\sigma}\mathbf{r}_{n+1}^{(k)} \cdot \Delta\sigma_{n+1}^{(k)} + \partial_{\mathbf{q}}\mathbf{r}_{n+1}^{(k)} \cdot \Delta\mathbf{q}_{n+1}^{(k)}\right)
\end{aligned} \tag{2.35}$$

Likewise,

$$\begin{aligned}
\mathbf{q}_{n+1}^{(k)} + \Delta\mathbf{q}_{n+1}^{(k)} &\approx \mathbf{q}_n + \Delta\lambda_{n+1}^{(k)}\mathbf{h}_{n+1}^{(k)} + \\
&\quad \delta\lambda_{n+1}^{(k)}\left(\mathbf{h}_{n+1}^{(k)} + \partial_{\sigma}\mathbf{h}_{n+1}^{(k)} \cdot \Delta\sigma_{n+1}^{(k)} + \partial_{\mathbf{q}}\mathbf{r}_{n+1}^{(k)} \cdot \Delta\mathbf{q}_{n+1}^{(k)}\right)
\end{aligned} \tag{2.36}$$

Linearizing σ results in,

$$\Delta\sigma_{n+1}^{(k)} = \mathbf{c}_{n+1}^{(k)} \cdot \left(-\Delta\epsilon_{n+1}^{\text{pl}(k)}\right) \tag{2.37}$$

18

Substituting this result into the previous two, and combining in a matrix format results in

$$\left\{ \begin{array}{c} \Delta\epsilon_{n+1}^{\text{pl}(k)} \\ \Delta\mathbf{q}_{n+1}^{(k)} \end{array} \right\} = \left[\begin{array}{cc} \left(\mathbf{c}_{n+1}^{(k)}\right)^{-1} & \mathbf{0} \\ \mathbf{0} & -\mathbf{I} \end{array} \right] \mathbf{A}_{n+1}^{(k)} \left(\mathbf{R}_{n+1}^{(k)} + \Delta\lambda_{n+1}^{(k)} \left\{ \begin{array}{c} \mathbf{r}_{n+1}^{(k)} \\ \mathbf{h}_{n+1}^{(k)} \end{array} \right\} \right) \quad (2.38)$$

where $\mathbf{A}_{n+1}^{(k)}$ is defined in (2.22) and $\mathbf{R}_{n+1}^{(k)}$ is defined in (2.18). In order to determine an expression for $\Delta\lambda_{n+1}^{(k)}$, we must linearize f about state k, viz.,

$$\begin{aligned} 0 = f_{n+1}^{(k+1)} &= f_{n+1}^{(k)} + \Delta f_{n+1}^{(k)} \\ &\approx f_{n+1}^{(k)} + \left[\begin{array}{cc} -\mathbf{c}_{n+1}^{(k)}\partial_{\boldsymbol{\sigma}} f_{n+1}^{(k)} & \partial_{\mathbf{q}} f_{n+1}^{(k)} \end{array} \right] \left\{ \begin{array}{c} \Delta\epsilon_{n+1}^{\text{pl}(k)} \\ \Delta\mathbf{q}_{n+1}^{(k)} \end{array} \right\} \\ &= f_{n+1}^{(k)} - \left[\begin{array}{cc} \partial_{\boldsymbol{\sigma}} f_{n+1}^{(k)} & \partial_{\mathbf{q}} f_{n+1}^{(k)} \end{array} \right] \mathbf{A}_{n+1}^{(k)} \times \\ &\qquad \left(\mathbf{R}_{n+1}^{(k)} + \Delta\lambda_{n+1}^{(k)} \left\{ \begin{array}{c} \mathbf{r}_{n+1}^{(k)} \\ \mathbf{h}_{n+1}^{(k)} \end{array} \right\} \right) \end{aligned} \quad (2.39)$$

Solving this expression for $\Delta\lambda_{n+1}^{(k)}$ yields (2.23).

2. The algorithm has a simple geometric interpretation in the case of perfect plasticity ($\mathbf{q} = \mathbf{0}$), linear elastic response ($\mathbf{c} = $ constant), and an associative flow rule ($\mathbf{h} = \partial_{\boldsymbol{\sigma}} f$). $\boldsymbol{\sigma}_{n+1}$ is the projection onto the yield surface of the trial elastic stress $\boldsymbol{\sigma}_{n+1}^{\text{trial}} = \partial_{\epsilon}\Psi\left(\epsilon_{n+1} - \epsilon_{n}^{\text{pl}}\right)$ taking as a metric the tensor $\mathbf{c}$ (see Figure 2.1). In summary, $\boldsymbol{\sigma}_{n+1}$ is the *closest point projection of $\boldsymbol{\sigma}_{n+1}^{\text{trial}}$ onto the yield surface in the energy norm*.

3. In the case of an associative flow rule, normality is enforced with respect to state $n + 1$.

19

4. The algorithm is fully implicit.

2.2 Rate-independent Anisotropic Elastic Damage Model

The starting point is the assumption that reinforced concrete can be suitably defined by elastic moduli. We note that nothing in the theory precludes these moduli from defining an anisotropic material. For example, the moduli could represent the anisotropy induced by the pattern and amount of reinforcement. One assumes in this case that the basic constitutive relation is given by

$$\boldsymbol{\sigma} = \mathbf{c}\boldsymbol{\epsilon} \tag{2.40}$$

Time differentiating the above equation one gets

$$\dot{\boldsymbol{\sigma}} = \mathbf{c}\dot{\boldsymbol{\epsilon}} + \dot{\mathbf{c}}\boldsymbol{\epsilon} \tag{2.41}$$

As opposed to classical plasticity, where a rate equation defines the evolution of the plastic strain, the proposed damage model contains an evolution law for the elastic moduli **c**.
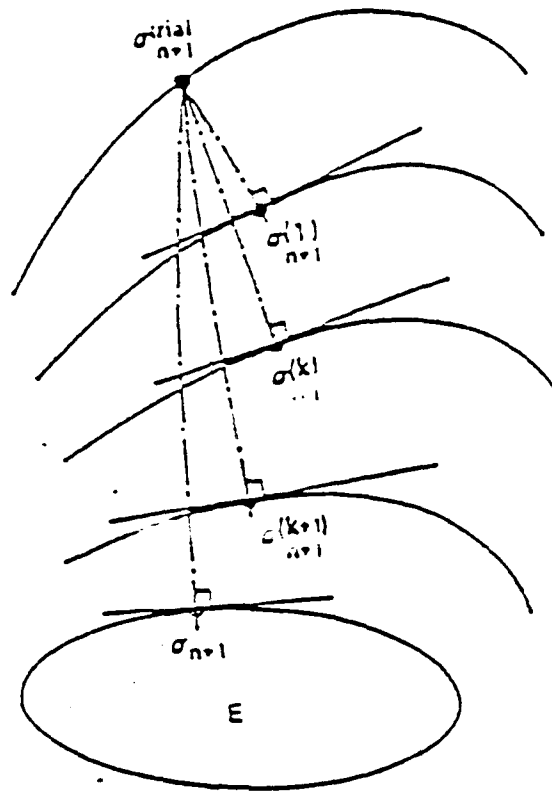
The following notation is introduced:

Figure 2.1: Conceptual representation of the elastic predictor-plastic return mapping algorithm for perfect plasticity (no hardening).

σ Stress tensor

ϵ Strain tensor

$\mathbf{c}$ Elastic moduli

α Strain-like internal variable

q Stress-like internal variable conjugate to α

ϕ Failure surface

f Stress dependent contribution to ϕ

ψ Total free energy function, $\psi(\epsilon, \mathbf{c}, \alpha) = \frac{1}{2}\epsilon \cdot \mathbf{c}\epsilon + \mathcal{H}(\alpha)$

$\mathcal{H}$ Surface-like energy such that $q = -\mathcal{H}'(\alpha)$

λ Consistency parameter

σ_f Material constant used in the definition of the failure surface

$\mathbf{N}$ Update direction given by $\mathbf{N} = \mathbf{c}\partial_{\sigma}\phi$

$\otimes$ Tensor product

The stress-dependent contribution f to the failure surface ϕ should not be confused with the yield surface employed in the theory of Box 1. As will become clear, the proposed model contains *no* plasticity, relying instead on an *elastic* constitutive relation combined with a failure surface.

The continuum damage model is then given by the following equations:

Box 2. *A small-deformation anisotropic elastic damage constitutive theory.*

Constitutive equation:

$$\boldsymbol{\sigma} = \mathbf{c}\boldsymbol{\epsilon} \tag{2.42}$$

Hardening law:

$$\dot{q} = -\dot{\alpha}\mathcal{H}'' \tag{2.43}$$

Damage evolution law:

$$\dot{\mathbf{c}} = -\dot{\lambda}\frac{\mathbf{c}\partial_{\boldsymbol{\sigma}}f \otimes \mathbf{c}\partial_{\boldsymbol{\sigma}}f}{\partial_{\boldsymbol{\sigma}}f \cdot \mathbf{c}\boldsymbol{\epsilon}} \tag{2.44}$$

Loading/unloading conditions:

$$\phi(\boldsymbol{\sigma}, \mathbf{q}) = f(\boldsymbol{\sigma}) + q - \sigma_f \leq 0 \tag{2.45}$$

$$\dot{\lambda} \geq 0 \tag{2.46}$$

$$\dot{\lambda}f(\boldsymbol{\sigma}, \mathbf{q}) = 0 \tag{2.47}$$

Remarks:

1. Since $\mathcal{H}$ is a function of α only, we employ the notation

$$\mathcal{H}' = \partial_\alpha \mathcal{H} \tag{2.48}$$

$$\mathcal{H}'' = \partial^2_{\alpha\alpha} \mathcal{H} \tag{2.49}$$

2. Because of the specific form chosen for the failure surface, one should note that

$$\partial_{\boldsymbol{\sigma}} \phi = \partial_{\boldsymbol{\sigma}} f \tag{2.50}$$

3. In a previous approach [11], damage was defined by a single scalar $d \in [0,1]$ that altered the elastic moduli in an isotropic fashion. Although this approach may be suitable for certain applications, the cracking of concrete intuitively gives rise to *anisotropic* damage. The model under consideration accomodates anisotropic changes in the elastic moduli (see equation (2.44)).

4. The total free energy consists of a classical elastic energy and a surface-like energy $\mathcal{H}$ that accounts for damage hardening/softening behavior.

5. Unlike classical elasticity, the elastic moduli c are treated as progressively degrading internal parameters; these are determined through their initial values — possibly anisotropic to account for reinforcement — and an evolution law which redefines them in specified directions according to the failure criterion. An illustration of this behavior is shown in Figure 2.2.
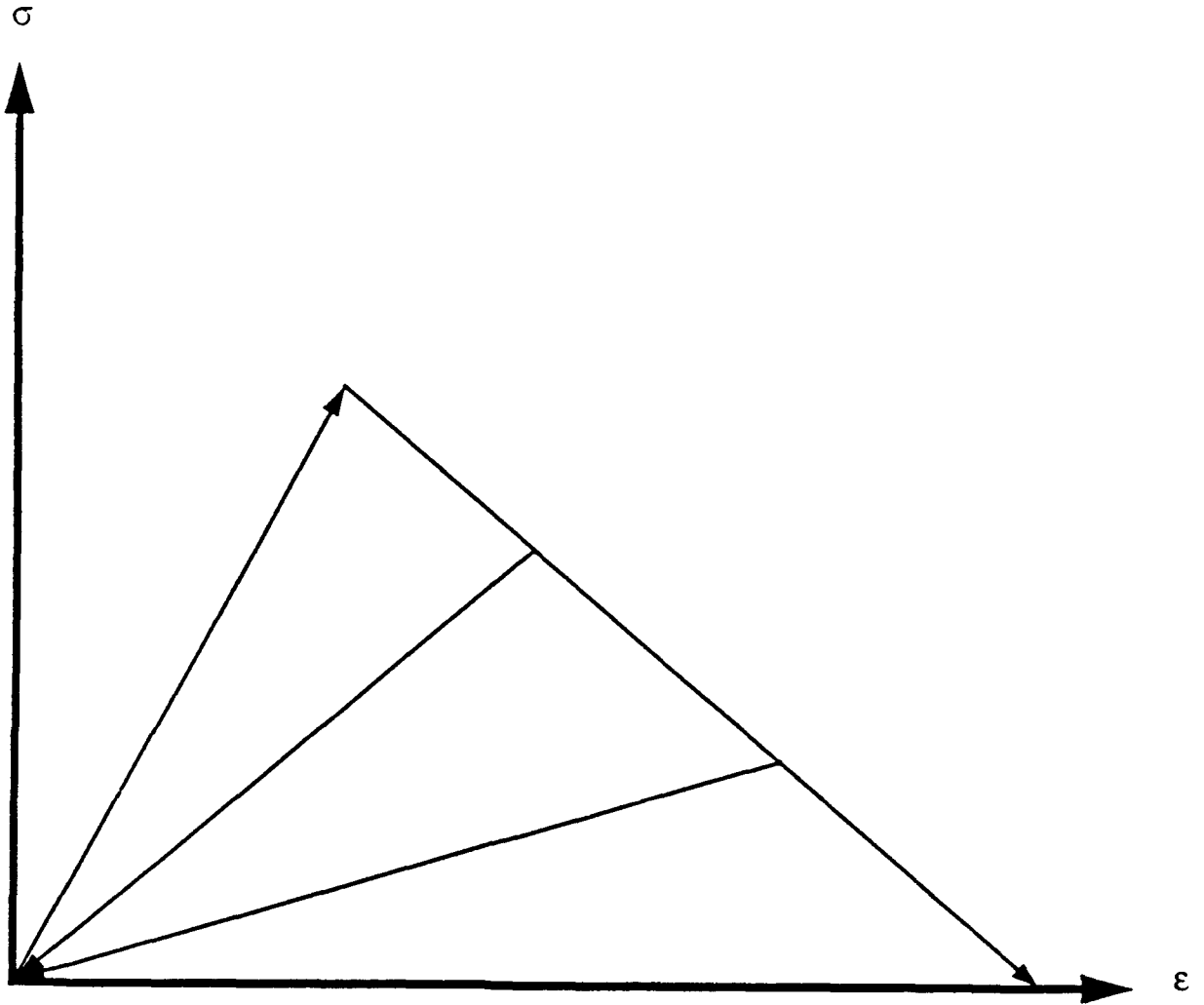
24

Figure 2.2: Stress-strain relation for a one-dimensional elastic damage model. The damage mechanism causes unloading at reduced values of the elastic modulus. Unloading occurs towards the origin.

6. The equations in Box 2 can be obtained by employing the principle of maximum dissipation (see [1.6.18]). We sketch the derivation below.

Time differentiating the free energy leads to

$$\dot{\psi} = \epsilon \cdot \mathbf{c}\dot{\epsilon} + \left[\frac{1}{2}\epsilon \cdot \dot{\mathbf{c}}\epsilon + \mathcal{H}'\dot{\alpha}\right] \tag{2.51}$$

By definition, the *dissipation function* $\mathcal{D}$ gives the rate of change in free energy due to changes in the inelastic internal variables. From (2.51), we get

$$\mathcal{D} = -\frac{1}{2}\epsilon \cdot \dot{\mathbf{c}}\epsilon - \mathcal{H}'\dot{\alpha} \tag{2.52}$$

Hence, the rate of change in the free energy is given by

$$\dot{\psi} = \mathbf{c}\dot{\epsilon} - \mathcal{D} \tag{2.53}$$

The second law of thermodynamics requires that, for all $\dot{\epsilon}$,

$$-\dot{\psi} + \sigma \cdot \dot{\epsilon} \geq 0 \tag{2.54}$$

Satisfaction of (2.54) can only be obtained if the following two conditions hold

$$\sigma = \mathbf{c}\epsilon \tag{2.55}$$

$$\mathcal{D} \geq 0 \tag{2.56}$$

Hence, the second law of thermodynamics combined with the form of the free energy assumed leads to two conclusions:

(a) The stress-strain relation takes on the usual elastic form, namely $\sigma = \mathbf{c}\epsilon$.

26

(b) The dissipation function $\mathcal{D}$ is non-negative.

In order to state the principle of maximum dissipation we introduce the set of admissible states $\mathcal{E}$,

$$\mathcal{E} = \{(\boldsymbol{\sigma}, q) \,|\, \phi(\boldsymbol{\sigma}, q) \leq 0\} \tag{2.57}$$

The *principle of maximum dissipation* then states that the dissipation function $\mathcal{D}$ is maximum subject to the constraint

$$(\boldsymbol{\sigma}, q) \in \mathcal{E} \tag{2.58}$$

Equivalenty, this can be phrased in terms of a minimization problem for $-\mathcal{D}$, namely

$$\min_{(\boldsymbol{\sigma}, q) \in \mathcal{E}} \quad (-\mathcal{D}) \tag{2.59}$$

If it were not for the constraint $\phi \leq 0$, the optimality conditions could be simply obtained by differentiating $-\mathcal{D}$ with respect to $\boldsymbol{\sigma}$ and q. This approach can still be utilized if one employs the method of Lagrange multipliers, which transforms the *constrained* minimization problem above into an *unconstrained* problem by appending to $-\mathcal{D}$ the constraint times a Lagrange multiplier $\dot{\lambda}$. This gives rise to a Lagrangian $\mathcal{L}$, defined by

$$\mathcal{L} = -\mathcal{D} + \dot{\lambda}\phi(\boldsymbol{\sigma}, q) \tag{2.60}$$

The optimality conditions are then given by

$$\partial_{\boldsymbol{\sigma}}\mathcal{L} = 0 \tag{2.61}$$

$$\partial_{q}\mathcal{L} = 0 \tag{2.62}$$

27

along with the Kuhn-Tucker conditions

$$\dot{\lambda} \geq 0 \qquad (2.63)$$

$$\phi(\boldsymbol{\sigma}, q) \leq 0 \qquad (2.64)$$

$$\dot{\lambda}\phi(\boldsymbol{\sigma}, q) = 0 \qquad (2.65)$$

In order to perform the differentiations in (2.61) and (2.62), we rewrite the dissipation function $\mathcal{D}$ as an explicit function of $\boldsymbol{\sigma}$ and q, obtaining

$$\mathcal{L} = \frac{1}{2}\boldsymbol{\sigma} \cdot \mathbf{c}^{-1}\dot{\mathbf{c}}\mathbf{c}^{-1}\boldsymbol{\sigma} - q\dot{\alpha} + \dot{\lambda}\left[f(\boldsymbol{\sigma}) + q - \sigma_f\right] \qquad (2.66)$$

Differentiation with respect to $\boldsymbol{\sigma}$ and q is now straightforward leading to

$$\dot{\mathbf{c}}\boldsymbol{\epsilon} = -\dot{\lambda}\mathbf{c}\partial_{\boldsymbol{\sigma}}f \qquad (2.67)$$

$$\dot{\alpha} = \dot{\lambda} \qquad (2.68)$$

Note that the consistency parameter λ can be interpreted as a Lagrange multiplier that forces $\boldsymbol{\sigma}$ and q to stay within the allowable region.

7. In view of (2.68), the hardening law (2.43) can be rewritten as

$$\dot{q} = -\dot{\lambda}\partial_{\alpha\alpha}^2\mathcal{H} \qquad (2.69)$$

8. During amage loading, $\dot{\phi} = 0$. From (2.45) one gets

$$\dot{\phi} = \partial_{\boldsymbol{\sigma}}f \cdot \dot{\boldsymbol{\sigma}} + \dot{q} \qquad (2.70)$$

28

Time differentiating the constitutive equation (2.42) and substituting into (2.70) leads to

$$\dot{\varphi} = \partial_{\boldsymbol{\sigma}} f \cdot (\mathbf{c}\dot{\boldsymbol{\epsilon}} + \dot{\mathbf{c}}\boldsymbol{\epsilon}) + \dot{q} \tag{2.71}$$

Substituting the hardening and damage evolution laws, equations (2.43) and (2.44), into (2.71) and setting $\dot{\varphi}$ to zero results in an explicit expression for the consistency parameter,

$$\dot{\lambda} = \frac{\partial_{\boldsymbol{\sigma}} f \cdot \mathbf{c}\dot{\boldsymbol{\epsilon}}}{\partial_{\boldsymbol{\sigma}} f \cdot \mathbf{c}\partial_{\boldsymbol{\sigma}} f + \mathcal{H}''} \tag{2.72}$$

9. The derivation of the expression for $\dot{\mathbf{c}}$, (2.44), deserves special attention. Assuming that $\dot{\mathbf{c}}$ is a rank-one tensor, the symmetry conditions

$$c_{ijkl} = c_{klij} = c_{jikl} = c_{ijlk} \tag{2.73}$$

and (2.67) imply the damage evolution law:

$$\dot{\mathbf{c}} = -\dot{\lambda}\frac{\mathbf{c}\partial_{\boldsymbol{\sigma}} f \otimes \mathbf{c}\partial_{\boldsymbol{\sigma}} f}{\partial_{\boldsymbol{\sigma}} f \cdot \mathbf{c}\boldsymbol{\epsilon}} \tag{2.74}$$

The rank-one assumption is the key to obtaining this simple expression. Note that (2.67) and (2.73) can be satisfied by infinitely many other definitions of $\dot{\mathbf{c}}$. This may be a worthwhile avenue of future research in that cracking and crushing may be amenable to more realistic treatment by appropriate generalizations of the definition of $\dot{\mathbf{c}}$. The subject of quasi-Newton updates may be relevant in this regard (see, e.g., Luenberger[14]) in that (2.67) has the form of the so-called quasi-Newton equation. It

29

should be possible using the methodology of quasi-Newton updates to satisfy (2.67),
(2.73), and other attributes deemed useful in the descrption of cracking, crushing,
bond-slip, etc.

2.3   Algorithms for the Rate-independent Anisotropic Elastic Damage Model

2.3.1   Fully Implicit Return Mapping Algorithm

A first attempt to integrate the above equations might employ a similar approach to
that used in the closest-point projection algorithm for plasticity. This would lead to the
following set of nonlinear equations:

$$\mathbf{c}_{n+1} = \mathbf{c}_n - \delta\lambda \frac{\mathbf{c}_{n+1}\partial_{\boldsymbol{\sigma}} f_{n+1} \otimes \mathbf{c}_{n+1}\partial_{\boldsymbol{\sigma}} f_{n+1}}{\partial_{\boldsymbol{\sigma}} f \cdot \mathbf{c}_{n+1}\epsilon_{n+1}} \tag{2.75}$$

$$\boldsymbol{\sigma}_{n+1} = \mathbf{c}_{n+1}\epsilon_{n+1} \tag{2.76}$$

$$q_{n+1} = -\mathcal{H}\left(\alpha_n + \delta\lambda\right) \tag{2.77}$$

In an elastic step, one has $\delta\lambda = 0$ and the solution of the above is obviously trivial.
However, if damage evolution occurs, to the above equations one adds

$$\phi\left(\boldsymbol{\sigma}_{n+1}, q_{n+1}\right) = 0 \tag{2.78}$$

Equations (2.75)-(2.78) amount to a fully implicit nonlinear system. One has
to solve *simultaneously* for $\mathbf{c}_{n+1}$, $\boldsymbol{\sigma}_{n+1}$, q_{n+1}, and $\delta\lambda$. Solving such a large nonlinear sys-

tem of equations at each integration point at each nonlinear iteration of a finite element
analysis appears impractical and alternative integration schemes are thus called for. Some
simplifications are described below.

2.3.2 Explicit/Implicit Methods

We consider the explicit integration of the elastic moduli while mantaining an implicit
integration for the other variables. This leads to the following system of equations

$$\sigma_{n+1}^{\text{trial}} = c_n \epsilon_{n+1} \tag{2.79}$$

$$c_{n+1} = c_n - \delta\lambda \frac{c_n \partial_{\sigma} f_{n+1}^{\text{trial}} \otimes c_n \partial_{\sigma} f_{n+1}^{\text{trial}}}{\partial_{\sigma} f_{n+1}^{\text{trial}} \cdot c_n \epsilon_{n+1}} \tag{2.80}$$

$$\sigma_{n+1} = c_{n+1} \epsilon_{n+1} \tag{2.81}$$

$$q_{n+1} = -\mathcal{H}'(\alpha_n + \delta\lambda) \tag{2.82}$$

$$\phi(\sigma_{n+1}, q_{n+1}) = 0 \tag{2.83}$$

The above system can be solved by the following algorithm:

31

Algorithm 2. *Explicit/implicit algorithm for the small-deformation elastic damage constitutive theory of Box 2.*

Step 1. Initialize:

$$\delta\lambda^{(0)} = 0 \tag{2.84}$$

$$\sigma_{n+1}^{(0)} = \sigma_{n+1}^{\text{trial}} = c_n \epsilon_{n+1} \tag{2.85}$$

$$N_{n+1}^{(0)} = c_n \cdot \partial_{\sigma} f_{n+1}^{(0)} \tag{2.86}$$

$$k = 0 \tag{2.87}$$

Step 2. Update stress and hardening parameters:

$$\sigma_{n+1}^{(k)} = \sigma_{n+1}^{\text{trial}} - \delta\lambda^{(k)} N_{n+1}^{(0)} \tag{2.88}$$

$$\alpha_{n+1}^{(k)} = \alpha_n + \delta\lambda^{(k)} \tag{2.89}$$

$$q_{n+1}^{(k)} = -\mathcal{H}'\left(\alpha_{n+1}^{(k)}\right) \tag{2.90}$$

Step 3. Check for failure and convergence:

$$\phi_{n+1}^{(k)} = f_{n+1}^{(k)} + q_{n+1}^{(k)} - \sigma_f \tag{2.91}$$

If $((k = 0$ and $\phi_{n+1}^{(k)} <$ TOL $)$ or $(|\phi_{n+1}^{(k)}| \leq$ TOL $))$ then

$$\sigma_{n+1} = \sigma_{n+1}^{(k)} \tag{2.92}$$

$$c_{n+1} = c_n - \delta\lambda^{(k)} \frac{N_{n+1}^{(0)} \otimes N_{n+1}^{(0)}}{N_{n+1}^{(0)} \cdot \epsilon_{n+1}} \tag{2.93}$$

$$\alpha_{n+1} = \alpha_{n+1}^{(k)} \tag{2.94}$$

return

endif

Step 4. Compute $\delta\lambda$-increment

$$D\phi_{n+1}^{(k)} = -\left[\partial_{\boldsymbol{\sigma}} f_{n+1}^{(k)} \cdot \mathbf{c}_n \mathbf{N}_{n+1}^{(0)} + \mathcal{H}''\left(\alpha_{n+1}^{(k)}\right)\right] \tag{2.95}$$

$$\delta\lambda^{(k+1)} = \delta\lambda^{(k)} - \phi_{n+1}^{(k+1)}/D\phi_{n+1}^{(k)} \tag{2.96}$$

Set $k = k + 1$ and go to Step 2.

Remarks:

1. The trial stress $\boldsymbol{\sigma}_{n+1}^{\text{trial}} = \boldsymbol{\sigma}_{n+1}^{(0)}$ is similar to that introduced in plasticity: the inelastic parameters are *frozen* at their previous values and the stress is updated with the *current* strain value.

2. Equation (2.88) is derived as follows:

$$
\begin{aligned}
\boldsymbol{\sigma}_{n+1} &= \mathbf{c}_{n+1}\epsilon_{n+1} \\
&= \mathbf{c}_n\epsilon_{n+1} + (\mathbf{c}_{n+1} - \mathbf{c}_n)\,\epsilon_{n+1} \\
&= \boldsymbol{\sigma}_{n+1}^{\text{trial}} + (\mathbf{c}_{n+1} - \mathbf{c}_n)\,\epsilon_{n+1}
\end{aligned}
\tag{2.97}
$$

The second term is replaced by a discrete version of (2.67), namely

$$(c_{n+1} - c_n) \epsilon_{n+1} = -\delta\lambda c_n \partial_{\sigma} f_{n+1}^{(0)} \tag{2.98}$$

3. The above system of equations contains a single scalar unknown $\delta\lambda$, a considerable simplification compared with the fully implicit system described previously. This single scalar unknown is the solution of (2.83), which can be written in the form

$$0 = \hat{\phi}(\delta\lambda) = f\left(\sigma_{n+1}^{\text{trial}} - \delta\lambda N_{n+1}^{(0)}\right) - \mathcal{H}'(\alpha_n + \delta\lambda) - \sigma_f \tag{2.99}$$

Step 4 of the algorithm amounts to a Newton iteration method for solving this nonlinear scalar equation.

4. Note that the update direction is held fixed at its initial value $N_{n+1}^{(0)}$. In an attempt to improve upon the accuracy of the explicit/implicit solution described above, we consider a variant below which, at each nonlinear iteration, recomputes the update direction $N = c\partial_{\sigma} f$.

34

Algorithm 3. *Updated explicit/implicit algorithm for the small-deformation anisotropic elastic damage constitutive theory of Box 2.*

Step 1. Initialize:

$$\delta\lambda^{(n)} = 0 \tag{2.100}$$

$$\sigma_{n+1}^{(0)} = \sigma_{n+1}^{\text{trial}} = \mathbf{c}_n \epsilon_{n+1} \tag{2.101}$$

$$\mathbf{N}_{n+1}^{(0)} = \mathbf{c}_n \partial_{\boldsymbol{\sigma}} f_{n+1}^{(0)} \tag{2.102}$$

$$\mathbf{c}_{n+1}^{(0)} = \mathbf{c}_n \tag{2.103}$$

$$k = 0 \tag{2.104}$$

Step 2. Update stress and hardening parameters:

$$\sigma_{n+1}^{(k)} = \sigma_{n+1}^{\text{trial}} - \delta\lambda^{(k)} \mathbf{N}_{n+1}^{(k)} \tag{2.105}$$

$$\alpha_{n+1}^{(k)} = \alpha_n + \delta\lambda^{(k)} \tag{2.106}$$

$$q_{n+1}^{(k)} = -\mathcal{H}'\left(\alpha_{n+1}^{(k)}\right) \tag{2.107}$$

Step 3. Check for failure and convergence:

$$\phi_{n+1}^{(k)} = f_{n+1}^{(k)} + q_{n+1}^{(k)} - \sigma_f \tag{2.108}$$

If $((k = 0$ and $\phi_{n+1}^{(k)} <$ TOL $)$ or $(|\phi_{n+1}^{(k)}| \leq$ TOL $))$ then

$$\sigma_{n+1} = \sigma_{n+1}^{(k)} \tag{2.109}$$

35

$$c_{n+1} = c_{n+1}^{(k)} \tag{2.110}$$

$$\alpha_{n+1} = \alpha_{n+1}^{(k)} \tag{2.111}$$

return

endif

Step 4. Compute $\delta\lambda$-increment:

$$D\phi_{n+1}^{(k)} = - \left[\partial_{\boldsymbol{\sigma}} f_{n+1}^{(k)} \cdot \mathbf{N}_{n+1}^{(k)} + \mathcal{H}'' \left(\alpha_{n+1}^{(k)} \right) \right] \tag{2.112}$$

$$\delta\lambda^{(k+1)} = \delta\lambda^{(k)} - \phi_{n+1}^{(k)} / D\phi_{n+1}^{(k)} \tag{2.113}$$

Step 5. Update return direction and moduli:

$$\mathbf{N}_{n+1}^{(k+1)} = c_{n+1}^{(k)} \partial_{\boldsymbol{\sigma}} f_{n+1}^{(k)} \tag{2.114}$$

$$c_{n+1}^{(k+1)} = c_n - \delta\lambda^{(k+1)} \frac{\mathbf{N}_{n+1}^{(k+1)} \otimes \mathbf{N}_{n+1}^{(k+1)}}{\epsilon_{n+1} \cdot \mathbf{N}_{n+1}^{(k+1)}} \tag{2.115}$$

Set $k = k + 1$ and go to Step 2.

Remarks:

1. Despite the explicit update in the return direction $\mathbf{N}$, the algorithm is implicit with

   respect to the solution of the (nonlinear) equation

$$\phi \left(\boldsymbol{\sigma}_{n+1}, q_{n+1} \right) = 0 \tag{2.116}$$

36

Analogous to (2.99), we write

$$0 = \hat{\phi}(\delta\lambda) = f\left(\sigma_{n+1}^{\text{trial}} - \delta\lambda N_{n+1}^{(k)}\right) - \mathcal{H}'(\alpha_n + \delta\lambda) - \sigma_f \tag{2.117}$$

Equation (2.112) follows from (2.117) by employing (2.105) and (2.106).

2. The update for the return direction, equation (2.114), is an attempt to approximate the implicit algorithm sketched in Section 2.3.1.

3. An important distinction between the present algorithm and the implicit algorithm of Section 2.3.1 is that here equation (2.75) is not necessarily satisfied by c_{n+1}.

4. The present algorithm represents an attractive balance between computational effort and implicitness. It is employed as a basis for subsequent developments within this report.

2.4   An Example: Elliptical Failure Surface in Pressure-Deviatoric Space

As an example of a typical application, we consider a failure surface given by

$$f(\sigma) = \frac{R^2}{S^2}(p - p_0)^2 + \|\text{dev}\sigma\|^2 - R^2 \tag{2.118}$$

$$p = -\text{tr}\sigma/3 \tag{2.119}$$

$$Q\sigma = \text{dev}\sigma = \sigma + pI \tag{2.120}$$

where R, S, and p_0 are material parameters.

Remarks:

1. $\mathbf{Q}$ is a projection operator that extracts the deviatoric part of a symmetric tensor. That it is indeed a projection can be seen from the fact that

$$\mathbf{Q}^2\sigma = \mathbf{Q}\sigma \qquad (2.121)$$

Along with $\mathbf{Q}$ we can introduce another projection operator $\mathbf{P}$,

$$\mathbf{P}\sigma = \mathrm{tr}\sigma\frac{\mathbf{I}}{3} \qquad (2.122)$$

where $\mathbf{I}$ stands for the identity matrix. Note that

$$\mathbf{P}\sigma + \mathbf{Q}\sigma = \sigma \qquad (2.123)$$

and that

$$\mathbf{PQ} = \mathbf{QP} = 0 \qquad (2.124)$$

2. The above failure surface represents an ellipse in $p - \mathrm{dev}\sigma$ space, with R being the semi-axis of the ellipse in the deviatoric plane and S the semi-axis in the pressure plane, as shown in Figure 2.3.

3. As mentioned in [11], if the cutting plane algorithm is employed, the failure surface has a preferred representation which, in the current case is

$$f(\sigma) = \sqrt{\frac{R^2}{S^2}(p - p_0)^2 + \|\mathrm{dev}\sigma\|^2 - R^2} \qquad (2.125)$$

38

4. p_0 is introduced in order to control the tensile resistance of the concrete model.

5. The failure surface above is isotropic. A more general surface of the Tsai-Wu type (see, e.g., Jones [12]) is given by

$$f(\boldsymbol{\sigma}) = \frac{R^2}{S^2}(p - p_0)^2 + \frac{1}{2}\mathbf{Q}\boldsymbol{\sigma} \cdot \mathbf{MQ}\boldsymbol{\sigma} - R^2 \qquad (2.126)$$

where the tensor $\mathbf{M}$ could account for anisotropic elastic behavior as that emanating from reinforcement. For simplicity in the exposition, we proceed with the surface described by (2.118). The generalization to (2.126) is straightforward.

Damage will be described according to the relation

$$\mathcal{H}(\alpha) = -H\alpha \qquad (2.127)$$

where H is assumed to be a positive constant. The negative sign is indicative of the presence of softening behavior attributable to crushing and/or cracking of concrete.

For a material characterized by (2.118), one can utilize Algorithm 3 in which

$$\partial_{\boldsymbol{\sigma}}f = -\frac{2}{3}\frac{R^2}{S^2}(p - p_0)\mathbf{I} + 2\mathbf{Q}\boldsymbol{\sigma} \qquad (2.128)$$

$$\mathcal{H}' = -H \qquad (2.129)$$

$$\mathcal{H}'' = 0 \qquad (2.130)$$

For the sake of completeness, Algorithm 3 is specialized to this case.
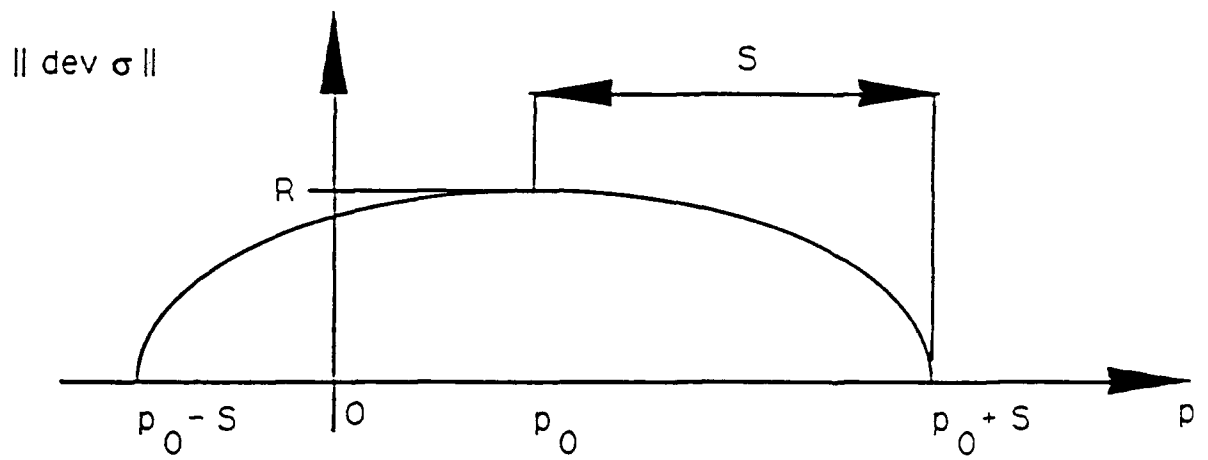
Figure 2.3: Elliptical damage surface in the pressure-deviatoric plane.

Algorithm 4. *Updated explicit/implicit algorithm for the small-deformation anisotropic elastic damage constitutive theory of Box 2 with assumed elliptical failure surface in pressure-deviator space and constant hardening modulus.*

Step 1. Initialize:

$$\delta\lambda^{(0)} = 0 \tag{2.131}$$

$$\boldsymbol{\sigma}_{n+1}^{(0)} = \boldsymbol{\sigma}_{n+1}^{\text{trial}} = \mathbf{c}_n \boldsymbol{\epsilon}_{n+1} \tag{2.132}$$

$$p_{n+1}^{(0)} = -\text{tr}\boldsymbol{\sigma}_{n+1}^{(0)}/3 \tag{2.133}$$

$$\text{dev}\boldsymbol{\sigma}_{n+1}^{(0)} = \boldsymbol{\sigma}_{n+1}^{(0)} + p_{n+1}^{(0)}\mathbf{I} \tag{2.134}$$

$$\mathbf{N}_{n+1}^{(0)} = 2\mathbf{c}_n \left[-\frac{1}{3}\frac{R^2}{S^2}\left(p_{n+1}^{(0)} - p_0\right)\mathbf{I} + \text{dev}\boldsymbol{\sigma}_{n+1}^{(0)} \right] \tag{2.135}$$

$$\mathbf{c}_{n+1}^{(0)} = \mathbf{c}_n \tag{2.136}$$

$$k = 0 \tag{2.137}$$

Step 2. Update stress and hardening parameter:

$$\boldsymbol{\sigma}_{n+1}^{(k)} = \boldsymbol{\sigma}_{n+1}^{\text{trial}} - \delta\lambda^{(k)}\mathbf{N}_{n+1}^{(k)} \tag{2.138}$$

$$p_{n+1}^{(k)} = -\text{tr}\boldsymbol{\sigma}_{n+1}^{(k)}/3 \tag{2.139}$$

$$\text{dev}\boldsymbol{\sigma}_{n+1}^{(k)} = \boldsymbol{\sigma}_{n+1}^{(k)} + p_{n+1}^{(k)}\mathbf{I} \tag{2.140}$$

$$\alpha_{n+1}^{(k)} = \alpha_n + \delta\lambda^{(k)} \tag{2.141}$$

41

Step 3. Check for failure and convergence:

$$\phi_{n+1}^{(k)} = \frac{R^2}{S^2}\left(p_{n+1}^{(k)} - p_0\right)^2 + \|\mathrm{dev}\,\sigma_{n+1}^{(k)}\|^2 - R^2 + H - \sigma_f \qquad (2.142)$$

If $((k = 0$ and $\phi_{n+1}^{(k)} < $ TOL $)$ or $(|\phi_{n+1}^{(k)}| \leq $ TOL $))$ then

$$\sigma_{n+1} = \sigma_{n+1}^{(k)} \qquad (2.143)$$

$$\mathbf{c}_{n+1} = \mathbf{c}_{n+1}^{(k)} \qquad (2.144)$$

$$\alpha_{n+1} = \alpha_{n+1}^{(k)} \qquad (2.145)$$

return

endif

Step 4. Compute $\delta\lambda$-increment:

$$D\phi_{n+1}^{(k)} = -2\left[-\frac{1}{3}\frac{R^2}{S^2}\left(p_{n+1}^{(k)} - p_0\right)\mathbf{I} + \mathrm{dev}\sigma_{n+1}^{(k)}\right]\cdot\mathbf{N}_{n+1}^{(k)} \qquad (2.146)$$

$$\delta\lambda^{(k+1)} = \delta\lambda^{(k)} - \phi_{n+1}^{(k)}/D\phi_{n+1}^{(k)} \qquad (2.147)$$

Step 5. Update moduli and return direction:

$$\mathbf{N}_{n+1}^{(k+1)} = 2\mathbf{c}_{n+1}^{(k)}\left[-\frac{1}{3}\frac{R^2}{S^2}\left(p_{n+1}^{(k)} - p_0\right)\mathbf{I} + \mathrm{dev}\sigma_{n+1}^{(k)}\right] \qquad (2.148)$$

$$\mathbf{c}_{n+1}^{(k+1)} = \mathbf{c}_n - \delta\lambda^{(k+1)}\frac{\mathbf{N}_{n+1}^{(k+1)} \otimes \mathbf{N}_{n+1}^{(k+1)}}{\epsilon_{n+1}\cdot\mathbf{N}_{n+1}^{(k+1)}} \qquad (2.149)$$

Set $k = k + 1$ and go to Step 2.

2.5 Rate-dependent Damage Model

The rate-dependent damage model can be obtained from the rate-independent model by means of a *viscous regularization* of the Perzyna type[11.16]. In this generalization, λ is replaced by $\langle \chi(\varphi) \rangle / \tau$, where χ is a non-dimensional function of φ. $\langle . \rangle$ denotes the Macaulay bracket, viz.

$$\langle x \rangle = \begin{cases} x & \text{If } x > 0 \\ 0 & \text{otherwise} \end{cases} \tag{2.150}$$

and τ is the relaxation time. Also, the damage loading/unloading conditions are dispensed with. As will be shown below, this model has the advantage of being trivially implemented in a finite element context.

The theory is summarized in Box 3.

Box 3. *A small-deformation anisotropic rate-dependent damage constitutive theory.*

Constitutive equation:

$$\boldsymbol{\sigma} = \mathbf{c}\boldsymbol{\epsilon} \tag{2.151}$$

Hardening law:

$$\dot{q} = -\frac{\langle \chi(\varphi) \rangle}{\tau} \mathcal{H}'' \tag{2.152}$$

Damage evolution law:

$$\dot{\mathbf{c}} = -\frac{\langle \chi(\phi) \rangle}{\tau} \frac{\mathbf{c}\partial_{\boldsymbol{\sigma}} f \otimes \mathbf{c}\partial_{\boldsymbol{\sigma}} f}{\partial_{\boldsymbol{\sigma}} f \cdot \mathbf{c}\boldsymbol{\epsilon}} \qquad (2.153)$$

Remarks:

1. Just as in viscoplasticity, the function χ may be taken to be

$$\chi(\phi) = (\text{sgn}\phi)(\phi/y)^N \qquad (2.154)$$

where y and N are positive constants, [11].

2.5.1 Algorithm for the Rate-dependent Damage Model

Integration of the equations in Box 3 can be done according to the following algorithm:

Algorithm 5. *Updated explicit/implicit algorithm for the small-deformation anisotropic elastic damage constitutive theory of Box 2, or rate-dependent damage constitutive theory of Box 3.*

Step 1. Initialize:

$$\text{lvisc} = \begin{cases} \text{true,} & \text{rate-dependent damage} & (\text{Box 3}) \\ \text{false,} & \text{elastic damage} & (\text{Box 2}) \end{cases}$$

44

lquit = false

$$\Delta t_{n+1} = t_{n+1} - t_n \tag{2.155}$$

$$\delta\lambda^{(0)} = 0 \tag{2.156}$$

$$t_{n+1}^{(0)} = t_n \tag{2.157}$$

$$\boldsymbol{\sigma}_{n+1}^{(0)} = \boldsymbol{\sigma}_{n+1}^{\text{trial}} = \mathbf{c}_n \boldsymbol{\epsilon}_{n+1} \tag{2.158}$$

$$\mathbf{N}_{n+1}^{(0)} = \mathbf{c}_n \partial_{\boldsymbol{\sigma}} f_{n+1}^{(0)} \tag{2.159}$$

$$\mathbf{c}_{n+1}^{(0)} = \mathbf{c}_n \tag{2.160}$$

$$k = 0 \tag{2.161}$$

Step 2. Update stress and hardening parameters:

$$\boldsymbol{\sigma}_{n+1}^{(k)} = \boldsymbol{\sigma}_{n+1}^{\text{trial}} - \delta\lambda^{(k)} \mathbf{N}_{n+1}^{(k)} \tag{2.162}$$

$$\alpha_{n+1}^{(k)} = \alpha_n + \delta\lambda^{(k)} \tag{2.163}$$

$$q_{n+1}^{(k)} = -\mathcal{H}'\left(\alpha_{n+1}^{(k)}\right) \tag{2.164}$$

Step 3. Check for failure and convergence:

$$\phi_{n+1}^{(k)} = f_{n+1}^{(k)} + q_{n+1}^{(k)} - \sigma_f \tag{2.165}$$

If $((k = 0$ and $\phi_{n+1}^{(k)} < $ TOL $)$ or

(lvisc = false and $|\phi_{n+1}^{(k)}| \leq$ TOL)) then lquit = true

If (lquit = true) then

$$\boldsymbol{\sigma}_{n+1} = \boldsymbol{\sigma}_{n+1}^{(k)} \tag{2.166}$$

$$\mathbf{c}_{n+1} = \mathbf{c}_{n+1}^{(k)} \qquad (2.167)$$

$$\alpha_{n+1} = \alpha_{n+1}^{(k)} \qquad (2.168)$$

return

endif

Step 4. Compute $\delta\lambda$-increment:

$$D\phi_{n+1}^{(k+1)} = - \left[\partial_{\boldsymbol{\sigma}} f_{n+1}^{(k)} \cdot \mathbf{N}_{n+1}^{(k)} + \mathcal{H}'' \left(\alpha_{n+1}^{(k)} \right) \right] \qquad (2.169)$$

If (lvisc = false) then

$$\delta\lambda^{(k+1)} = \delta\lambda^{(k)} - \phi_{n+1}^{(k)} / D\phi_{n+1}^{(k)} \qquad (2.170)$$

else

$$\bar{t}_{n+1}^{(k)} = -\frac{\tau}{\chi_{n+1}'^{(k)} D\phi_{n+1}^{(k)}} \qquad (2.171)$$

$$\Delta t_{n+1}^{(k)} = \bar{t}_{n+1}^{(k)} \left[1 - \exp \left(\frac{-\Delta t_{n+1}}{\bar{t}_{n+1}^{(k)}} \right) \right] \qquad (2.172)$$

$$t_{n+1}^{(k+1)} = t_{n+1}^{(k)} + \Delta t_{n+1}^{(k)} \qquad (2.173)$$

If $(t_{n+1}^{(k+1)} - t_{n+1} \geq 0)$ then

$$\Delta t_{n+1}^{(k)} = \Delta t_{n+1}^{(k)} - \left(t_{n+1}^{(k+1)} - t_{n+1} \right) \qquad (2.174)$$

lquit = true

endif

$$\delta\lambda^{(k+1)} = \delta\lambda^{(k)} + \Delta t_{n+1}^{(k)} \chi_{n+1}^{(k)} / \tau \qquad (2.175)$$

endif

Step 5. Update return direction and moduli:

$$\mathbf{N}_{n+1}^{(k+1)} = c_{n+1}^{(k)} \partial_{\boldsymbol{\sigma}} f_{n+1}^{(k)} \tag{2.176}$$

$$c_{n+1}^{(k+1)} = c_n - \delta\lambda^{(k+1)} \frac{\mathbf{N}_{n+1}^{(k+1)} \otimes \mathbf{N}_{n+1}^{(k+1)}}{\epsilon_{n+1} \cdot \mathbf{N}_{n+1}^{(k+1)}} \tag{2.177}$$

Set $k = k + 1$ and go to Step 2.

Remarks:

1. As discussed in [11], the approach taken herein obviates the issue of stability by automatically defining *a priori* stable subincremental time steps within the context of the updated implicit/explicit algorithm. The reader is encouraged to note the similarities between the subincrementation strategy described in Algorithm 5 and the one in [11], as applied to the cutting plane algorithm.

Chapter 3

Plane Stress Models — Applications to Plates and Shells

The application of the damage models described previously leads to a trivial implementation in three-dimensional geometries. Evidently, one might attempt to model *thick* shells and/or plates with three-dimensional elements; however, as *the shell gets thinner, the* cost of three-dimensional analysis, and numerical difficulties engendered by thin, three-dimensional elements, suggest the use of shell structural elements.

3.1 Plane Stress Algorithm for the Rate-independent Anisotropic Elastic Damage Model

A common feature of the structural plate and shell elements is the *zero normal stress* (ZNS) constraint which, in the two-dimensional case, is equivalent to a plane stress formulation.

A general approach for the analysis of plane stress problems is based upon the introduction of ϵ_{33} as an independent variable, where the *third* direction is normal to the plane of interest. Solution of the resulting nonlinear system of equations can be obtained by introducing the ZNS constraint as an additional condition to be satisfied:

$$\sigma_{33} = 0 \tag{3.1}$$

One can easily modify Algorithm 3 by noting that the ZNS constraint can be written as

$$\left(c_n \epsilon_{n+1}^{(k+1)} \right) \cdot e_{33} - \delta\lambda^{(k+1)} N_{n+1}^{(k)} \cdot e_{33} = 0 \tag{3.2}$$

where e_{33} stands for the unit tensor in the 33-direction, namely

$$e_{33} = \begin{bmatrix} 0 & 0 & 0 \\ 0 & 0 & 0 \\ 0 & 0 & 1 \end{bmatrix} \tag{3.3}$$

Hence, the implicit computation of $\delta\lambda^{(k+1)}$ is done in conjunction with the computation of $\epsilon_{33}^{(k+1)}$. A complete plane stress algorithm is then given as follows:

Algorithm 6. *Updated explicit/implicit plane stress algorithm for the small-deformation anisotropic elastic damage constitutive theory of Box 2.*

Step 1. Initialize:

$$\delta\lambda^{(0)} = 0 \tag{3.4}$$

$$\epsilon = \epsilon_{n+1} \tag{3.5}$$

$$\epsilon_{33}^{(0)} = -\frac{c_{n.3311}\epsilon_{11} + c_{n.3322}\epsilon_{22} + 2c_{n.3312}\epsilon_{12} + 2c_{n.3323}\epsilon_{23} + 2c_{n.3313}\epsilon_{13}}{c_{n.3333}} \tag{3.6}$$

$$\boldsymbol{\sigma}_{n+1}^{(0)} = \boldsymbol{\sigma}_{n+1}^{\text{trial}} = \mathbf{c}_n\boldsymbol{\epsilon}_{n+1} \tag{3.7}$$

$$\mathbf{N}_{n+1}^{(0)} = \mathbf{c}_n\partial\boldsymbol{\sigma}f_{n+1}^{(0)} \tag{3.8}$$

$$\mathbf{c}_{n+1}^{(0)} = \mathbf{c}_n \tag{3.9}$$

$$k = 0 \tag{3.10}$$

Step 2. Update stress and hardening parameter:

$$\boldsymbol{\sigma}_{n+1}^{(k)} = \mathbf{c}_n\boldsymbol{\epsilon}_{n+1}^{(k)} - \delta\lambda^{(k)}\mathbf{N}_{n+1}^{(k)} \tag{3.11}$$

$$\alpha_{n+1}^{(k)} = \alpha_n + \delta\lambda^{(k)} \tag{3.12}$$

$$q_{n+1}^{(k)} = -\mathcal{H}'\left(\alpha_{n+1}^{(k)}\right) \tag{3.13}$$

Step 3. Check for failure and convergence:

$$\phi_{n+1}^{(k)} = f_{n+1}^{(k)} + q_{n+1}^{(k)} - \sigma_f \tag{3.14}$$

If $((k = 0$ and $\phi_{n+1}^{(k)} < \text{TOL}_1)$ or

$(|\phi_{n+1}^{(k)}| \leq \text{TOL}_1$ and $|\sigma_{n+1,33}^{(k)}| < \text{TOL}_2))$ then

$$\boldsymbol{\sigma}_{n+1} = \boldsymbol{\sigma}_{n+1}^{(k)} \tag{3.15}$$

$$\mathbf{c}_{n+1} = \mathbf{c}_{n+1}^{(k)} \tag{3.16}$$

$$\alpha_{n+1} = \alpha_{n+1}^{(k)} \tag{3.17}$$

return

50

endif

Step 4. Update $\delta\lambda$ and ϵ_{33}:

$$\left\{ \begin{array}{c} \delta\lambda^{(k+1)} \\ \epsilon_{33}^{(k+1)} \end{array} \right\} = \left\{ \begin{array}{c} \delta\lambda^{(k)} \\ \epsilon_{33}^{(k)} \end{array} \right\} -$$

$$\left[\begin{array}{cc} -\left(\partial_{\boldsymbol{\sigma}} f_{n+1}^{(k)} \cdot \mathbf{N}_{n+1}^{(k)} + \mathcal{H}''\left(\alpha_{n+1}^{(k)}\right) \right) & \left[\mathbf{c}_n \partial_{\boldsymbol{\sigma}} f_{n+1}^{(k)} \right]_{33} \\ -N_{n+1,33}^{(k)} & c_{n,3333} \end{array} \right]^{-1} \left\{ \begin{array}{c} \phi_{n+1}^{(k)} \\ \sigma_{n+1,33}^{(k)} \end{array} \right\} \quad (3.18)$$

Step 5. Update return direction and moduli:

$$\mathbf{N}_{n+1}^{(k+1)} = \mathbf{c}_{n+1}^{(k)} \partial_{\boldsymbol{\sigma}} f_{n+1}^{(k)} \tag{3.19}$$

$$\mathbf{c}_{n+1}^{(k+1)} = \mathbf{c}_n - \delta\lambda^{(k+1)} \frac{\mathbf{N}_{n+1}^{(k+1)} \otimes \mathbf{N}_{n+1}^{(k+1)}}{\epsilon_{n+1}^{(k+1)} \cdot \mathbf{N}_{n+1}^{(k+1)}} \tag{3.20}$$

Set $k = k + 1$ and go to Step 2.

Remarks:

1. Except in the 33-component, which is updated to satisfy the ZNS constraint, $\epsilon_{n+1}^{(k+1)}$ is identically equal to $\epsilon = \epsilon_{n+1}$,

2. Even though the traditional plane stress analysis does not contain the transverse shear stresses and strains, they were included in the analysis here so the algorithm can be applied to thick plates and shells, where these quantities are important. Likewise, the preceding algorithm may be reduced to the traditional case by omitting the transverse stresses and strains.

51

3. The algorithm allows for different tolerances in the satisfaction of each of the constraints. namely TOL_1 for the failure surface. and TOL_2 for the ZNS constraint.

4. The 2×2 system of equations one solves in Step 3 reflects the satisfaction of the two scalar constraints.

$$\phi \left[c_n \epsilon_{n+1}^{(k+1)} - \delta\lambda^{(k+1)} \mathbf{N}_{n+1}^{(k)}, -\mathcal{H}' \left(\alpha_n + \delta\lambda^{(k+1)} \right) \right] =$$

$$h_1 \left(\delta\lambda^{(k+1)}, \epsilon_{n+1,33}^{(k+1)} \right) = h_1^{(k+1)} = 0 \tag{3.21}$$

$$\left(c_n \epsilon_{n+1}^{(k+1)} \right) \cdot \mathbf{e}_{33} - \delta\lambda^{(k+1)} \mathbf{N}_{n+1}^{(k)} \cdot \mathbf{e}_{33} =$$

$$h_2 \left(\delta\lambda^{(k+1)}, \epsilon_{n+1,33}^{(k+1)} \right) = h_2^{(k+1)} = 0 \tag{3.22}$$

Standard application of Newton's method to the above two equations leads to

$$\begin{bmatrix} \partial_{\delta\lambda} h_1 & \partial_{\epsilon_{n+1,33}} h_1 \\ \partial_{\delta\lambda} h_2 & \partial_{\epsilon_{n+1,33}} h_2 \end{bmatrix}^{(k)} \left\{ \begin{array}{c} \delta\lambda^{(k+1)} - \delta\lambda^{(k)} \\ \epsilon_{n+1,33}^{(k+1)} - \epsilon_{n+1,33}^{(k)} \end{array} \right\} = \left\{ \begin{array}{c} h_1^{(k)} \\ h_2^{(k)} \end{array} \right\} \tag{3.23}$$

Differentiating (3.21) and (3.22) we get

$$\partial_{\delta\lambda} h_1 = - \left(\partial_{\boldsymbol{\sigma}} f_{n+1}^{(k)} \cdot \mathbf{N}_{n+1}^{(k)} + \mathcal{H}'' \left(\alpha_{n+1}^{(k)} \right) \right) \tag{3.24}$$

$$\partial_{\epsilon_{n+1,33}} h_1 = \left[c_n \partial_{\boldsymbol{\sigma}} f_{n+1}^{(k)} \right]_{33} \tag{3.25}$$

$$\partial_{\delta\lambda} h_2 = -N_{n+1,33}^{(k)} \tag{3.26}$$

$$\partial_{\epsilon_{n+1,33}} h_2 = c_{n,3333} \tag{3.27}$$

Combining (3.23) to (3.27) leads to the final expression in Step 4. equation (3.18).

3.2 Plane Stress Algorithm for the Rate-dependent Damage Model

In this Section we present an algorithm which incorporates the plane stress constraint in the rate-dependent damage constitutive theory. Our approach combines features of Algorithms 5 and 6. In the absence of rate-dependent effects, the algorithm reduces identically to the plane stress elastic damage case, namely Algorithm 6. The procedure is given as follows:

Algorithm 7. *Updated explicit/implicit plane stress algorithm for the small-deformation anisotropic elastic damage constitutive theory of Box 2, or rate-dependent damage constitutive theory of Box 3.*

Step 1. Initialize:

$$\text{lvisc} = \begin{cases} \text{true,} & \text{rate-dependent damage} \quad \text{(Box 3)} \\ \text{false,} & \text{elastic damage} \quad\quad\quad \text{(Box 2)} \end{cases}$$

$$\text{lquit} = \text{false}$$

$$\Delta t_{n+1} = t_{n+1} - t_n \tag{3.28}$$

$$t^{(0)}_{n+1} = t_n \tag{3.29}$$

$$\delta\lambda^{(0)} = 0 \tag{3.30}$$

$$\epsilon = \epsilon_{n+1} \tag{3.31}$$

$$\epsilon_{33}^{(0)} = -\frac{c_{n,3311}\epsilon_{11} + c_{n,3322}\epsilon_{22} + 2c_{n,3312}\epsilon_{12} + 2c_{n,3323}\epsilon_{23} + 2c_{n,3313}\epsilon_{13}}{c_{n,3333}} \qquad (3.32)$$

$$\sigma_{n+1}^{(0)} = \sigma_{n+1}^{\text{trial}} = \mathbf{c}_n \epsilon_{n+1} \qquad (3.33)$$

$$\mathbf{N}_{n+1}^{(0)} = \mathbf{c}_n \partial_{\boldsymbol{\sigma}} f_{n+1}^{(0)} \qquad (3.34)$$

$$\mathbf{c}_{n+1}^{(0)} = \mathbf{c}_n \qquad (3.35)$$

$$k = 0 \qquad (3.36)$$

Step 2. Update stress and hardening parameter:

$$\sigma_{n+1}^{(k)} = \mathbf{c}_n \epsilon_{n+1}^{(k)} - \delta\lambda^{(k)} \mathbf{N}_{n+1}^{(k)} \qquad (3.37)$$

$$\alpha_{n+1}^{(k)} = \alpha_n + \delta\lambda^{(k)} \qquad (3.38)$$

$$q_{n+1}^{(k)} = -\mathcal{H}'\left(\alpha_{n+1}^{(k)}\right) \qquad (3.39)$$

Step 3. Check for failure and convergence:

$$\phi_{n+1}^{(k)} = f_{n+1}^{(k)} + q_{n+1}^{(k)} - \sigma_f \qquad (3.40)$$

If $((k = 0$ and $\phi_{n+1}^{(k)} < \text{TOL}_1)$ or

(lvisc = false and $|\phi_{n+1}^{(k)}| \le \text{TOL}_1$ and

$|\sigma_{n+1,33}^{(k)}| < \text{TOL}_2))$ then lquit = true

If (lquit = true) then

$$\sigma_{n+1} = \sigma_{n+1}^{(k)} \qquad (3.41)$$

$$\mathbf{c}_{n+1} = \mathbf{c}_{n+1}^{(k)} \qquad (3.42)$$

$$\alpha_{n+1} = \alpha_{n+1}^{(k)} \qquad (3.43)$$

return

endif

Step 4. Update $\delta\lambda$ and ϵ_{33}:

$$D\phi_{n+1}^{(k)} = -\left[\partial_{\boldsymbol{\sigma}} f_{n+1}^{(k)} \cdot \mathbf{N}_{n+1}^{(k)} + \mathcal{H}''\left(\alpha_{n+1}^{(k)}\right)\right] \tag{3.44}$$

If (lvisc = false) then

$$\left\{\begin{array}{c} \delta\lambda^{(k+1)} \\ \epsilon_{33}^{(k+1)} \end{array}\right\} = \left\{\begin{array}{c} \delta\lambda^{(k)} \\ \epsilon_{33}^{(k)} \end{array}\right\} -$$
$$\left[\begin{array}{cc} D\phi_{n+1}^{(k)} & \left[\mathbf{c}_n \partial_{\boldsymbol{\sigma}} f_{n+1}^{(k)}\right]_{33} \\ -N_{n+1,33}^{(k)} & c_{n,3333} \end{array}\right]^{-1} \left\{\begin{array}{c} \phi_{n+1}^{(k)} \\ \sigma_{n+1,33}^{(k)} \end{array}\right\} \tag{3.45}$$

else

$$\bar{t}_{n+1}^{(k)} = -\frac{\tau}{\chi_{n+1}^{\prime(k)} D\phi_{n+1}^{(k)}} \tag{3.46}$$

$$\Delta t_{n+1}^{(k)} = \bar{t}_{n+1}^{(k)}\left[1 - \exp\left(\frac{-\Delta t_{n+1}}{\bar{t}_{n+1}^{(k)}}\right)\right] \tag{3.47}$$

$$t_{n+1}^{(k+1)} = t_{n+1}^{(k)} + \Delta t_{n+1}^{(k)} \tag{3.48}$$

If $(t_{n+1}^{(k+1)} - t_{n+1} \geq 0)$ then

$$\Delta t_{n+1}^{(k)} = \Delta t_{n+1}^{(k)} - \left(t_{n+1}^{(k+1)} - t_{n+1}\right) \tag{3.49}$$

lquit = true

endif

$$\delta\lambda^{(k+1)} = \delta\lambda^{(k)} + \Delta t_{n+1}^{(k)}\chi_{n+1}^{(k)}/\tau \tag{3.50}$$

$$\epsilon_{33}^{(k+1)} = -\frac{c_{n,3311}\epsilon_{11} + c_{n,3322}\epsilon_{22} + 2c_{n,3312}\epsilon_{12} + 2c_{n,3323}\epsilon_{23} + 2c_{n,3313}\epsilon_{13}}{c_{n,3333}} +$$
$$\frac{\delta\lambda^{(k+1)}N_{n+1,33}^{(k)}}{c_{n,3333}} \tag{3.51}$$

55

endif

Step 5. Update return direction and moduli:

$$\mathbf{N}_{n+1}^{(k+1)} = \mathbf{c}_{n+1}^{(k)} \partial \boldsymbol{\sigma} f_{n+1}^{(k)} \tag{3.52}$$

$$\mathbf{c}_{n+1}^{(k+1)} = \mathbf{c}_n - \delta\lambda^{(k+1)} \frac{\mathbf{N}_{n+1}^{(k+1)} \otimes \mathbf{N}_{n+1}^{(k+1)}}{\boldsymbol{\epsilon}_{n+1}^{(k+1)} \cdot \mathbf{N}_{n+1}^{(k+1)}} \tag{3.53}$$

Set $k = k + 1$ and go to Step 2.

Remarks:

1. Note that with the introduction of the flag "lvisc", Algorithm 7 can be employed for both elastic *and* rate-dependent damage.

2. Because $\delta\lambda^{(k+1)}$ is explicitly computed, in the rate-dependent case — see (3.50) — the evaluation of $\epsilon_{33}^{(k+1)} = \epsilon_{n+1,33}^{(k+1)}$ is also trivially obtained through use of the constitutive relation, equation (3.51).

3.3   Applications to Plates and Shells

The above algorithm can be naturally employed in the analysis of structural elements like plates and shells. An excellent source of information concerning three-dimensional continuum based shell/plate formulations is Stanley[21]. Other works pertinent to the

present subject are [16-18]. Because of the completeness of [21], only major features of the theory relevant to the present discussion will be recalled.

1. The shell element is obtained by degenerating a three-dimensional element with linear displacement variation through the thickenss. Two assumptions are made that distinguish continuum based shell elements from regular three-dimensional elements:

Straight Normals. This assumption is expressed by the equation

$$\mathbf{x}\left(\xi, \eta, z\right) = \bar{\mathbf{x}}\left(\xi, \eta\right) + z\hat{\mathbf{x}}\left(\xi, \eta\right) \tag{3.54}$$

where ξ and η stand for *parent domain* curvilinear coordinates while z is a (linear) through-thickness coordinate. We note that z is usually written as

$$z\left(\xi, \eta\right) = \left(\zeta - \bar{\zeta}\right) h/2 \tag{3.55}$$

where $\zeta \in [-1, 1]$ and $\bar{\zeta}$ locates the reference surface. h is the shell thickness.

Inextensible Normals. This can be described incrementally by the relations

$$\Delta\mathbf{u}\left(\xi, \eta, z\right) = \Delta\bar{\mathbf{u}}\left(\xi, \eta\right) + z\Delta\hat{\mathbf{u}}\left(\xi, \eta\right) \tag{3.56}$$

$$\Delta\hat{\mathbf{u}} \cdot \hat{\mathbf{x}} = 0 \tag{3.57}$$

However, in practice it is necessary to maintain the inextensibility condition exactly. This can be achieved by various means. For example, one can use $\Delta\hat{\mathbf{u}}$ to define an increment of angle of rotation and thereby construct an orthogonal rotation matrix to transform the normal rigidly[21], or one can use a radial

57

projection algorithm (e.g., Hughes and Liu [7]).

2. An orthogonal local coordinate system $\left(\mathbf{e}_1^l, \mathbf{e}_2^l, \mathbf{e}_3^l\right)$ referred to as the *laminar* system is introduced. Its most important attribute is that $\mathbf{e}_3^l$ is normal to the surface $\zeta =$ constant at each point in the *current* configuration. By expressing the stress tensor in this laminar system, the constitutive algorithms introduced above for the plane stress problem can be easily implemented.

3. The continuum based approach has the distinct advantage that rigorous finite deformational constitutive theories can be readily utilized; one is only left with the ZNS constraint to deal with as described above.

Chapter 4

Extension to Multiple Failure Surfaces

4.1   Rate-independent Anisotropic Elastic Damage Model

Because of the importance of models that need to accomodate multiple failure surfaces (e.g., the cap model [11] or those proposed by Hashin [4]), we present extensions of the preceding ideas to multiple surfaces [20,18].

A theory for a model whose failure surface is defined by m smooth surfaces is described in Box 4. The free index "A" is understood to take on the values $1, 2, \ldots, m$.

Box 4. *A multiple failure surface, small-deformation anisotropic elastic damage constitutive theory.*

Constitutive equation:

$$\boldsymbol{\sigma} = \mathbf{c}\boldsymbol{\epsilon} \tag{4.1}$$

Hardening law:

$$\dot{q}_A = -\sum_{B=1}^{m} \dot{\alpha}_B \partial^2_{\alpha_A \alpha_B} \mathcal{H} \tag{4.2}$$

Damage evolution law:

$$\dot{\mathbf{c}} = -\sum_{B=1}^{m} \dot{\lambda}^B \frac{\mathbf{c}\partial_{\boldsymbol{\sigma}} f_B \otimes \mathbf{c}\partial_{\boldsymbol{\sigma}} f_B}{\partial_{\boldsymbol{\sigma}} f_B \cdot \mathbf{c}\boldsymbol{\epsilon}} \tag{4.3}$$

Loading/unloading conditions:

$$\phi_A = f_A + q_A - \sigma_A \leq 0 \tag{4.4}$$

$$\dot{\lambda}_A \geq 0 \tag{4.5}$$

$$\dot{\lambda}_A f_A\left(\boldsymbol{\sigma}, q_A\right) = 0 \tag{4.6}$$

60

Remarks:

1. $\mathcal{H}$ is a function of m independent strain-like variables $\alpha_1, \alpha_2, \ldots, \alpha_m$. Thus, the total free energy may be written as

$$\psi\left(\boldsymbol{\epsilon}, \mathbf{c}, \alpha_1, \alpha_2, \ldots, \alpha_m\right) = \frac{1}{2}\boldsymbol{\epsilon} \cdot \mathbf{c}\boldsymbol{\epsilon} + \mathcal{H}\left(\alpha_1, \alpha_2, \ldots, \alpha_m\right) \tag{4.7}$$

2. The q_A's are defined by

$$q_A = -\partial_{\alpha_A}\mathcal{H} \tag{4.8}$$

3. The principle of maximum dissipation is invoked as for the theory of Box 2. In the present context, this leads to

$$\mathbf{c}\dot{\boldsymbol{\epsilon}} = -\sum_{B=1}^{m} \dot{\lambda}^B \mathbf{c}\partial_{\boldsymbol{\sigma}} f_B \tag{4.9}$$

$$\dot{\alpha}_A = \dot{\lambda}^A \tag{4.10}$$

4. The consistency parameters $\dot{\lambda}^A$ can be obtained by time differentiating the damage functions ϕ_A and setting the resulting expression to zero. From (4.1), (4.2), (4.4) and (4.10) we get

$$\dot{\phi}_A = \partial_{\boldsymbol{\sigma}} f_A \cdot (\mathbf{c}\dot{\boldsymbol{\epsilon}} + \dot{\mathbf{c}}\boldsymbol{\epsilon}) - \sum_{B=1}^{m} \dot{\lambda}^B \partial^2_{\alpha_A \alpha_B} \mathcal{H} = 0 \tag{4.11}$$

Substituting (4.9) into (4.11) leads to the final system of equations for $\dot{\lambda}^A$,

$$\left\{\dot{\lambda}^A\right\} = \left[\partial_{\boldsymbol{\sigma}} f_A \cdot \mathbf{c}\partial_{\boldsymbol{\sigma}} f_B + \partial^2_{\alpha_A \alpha_B} \mathcal{H}\right]^{-1} \left\{\partial_{\boldsymbol{\sigma}} f_B \cdot \mathbf{c}\dot{\boldsymbol{\epsilon}}\right\} \tag{4.12}$$

61

5. From symmetry arguments, and by assuming that each surface contributes a rank-one update to the rate of change of the elastic moduli, one obtains

$$\dot{\mathbf{c}} = -\sum_{B=1}^{m} \dot{\lambda}^B \frac{\mathbf{c}\partial_{\boldsymbol{\sigma}} f_B \otimes \mathbf{c}\partial_{\boldsymbol{\sigma}} f_B}{\partial_{\boldsymbol{\sigma}} f_B \cdot \mathbf{c}\epsilon} \tag{4.13}$$

4.1.1 Algorithm for the Rate-independent Anisotropic Elastic Damage Model

We consider an integration scheme similar to that of Algorithm 3; however, because the active surfaces (i.e., those for which $\phi_A > 0$) are not known *a priori*, a new procedure needs to be developed. To this end we introduce the set of active surfaces at iteration k,

$$J_{\text{act}}^{(k)} = \left\{ A \mid \phi_A^{(k)} > 0 \right\} \tag{4.14}$$

The procedure is then defined by the following steps:

1. Let $J_{\text{act}}^{(k)}$ be the set of active surfaces at the k-th iteration. Compute increments $\delta\lambda^{A(k)}$, $A \in J_{\text{act}}^{(k)}$, by employing an approach similar to that of Algorithm 3, as described below.

2. Update $\delta\lambda^{A(k)}$ by setting

$$\delta\lambda^{A(k+1)} = \delta\lambda^{A(k)} + \Delta\lambda^{A(k)} \tag{4.15}$$

and check the sign of $\delta\lambda^{A(k+1)}$. If negative, drop constraint A from the active set and restart the iteration. Otherwise proceed.

62

The algorithm can be stated as follows:

Algorithm 8. *Updated explicit/implicit algorithm for the multiple failure surface, small-deformation anisotropic elastic damage constitutive theory of Box 4.*

Step 1. Initialize:

$$\delta\lambda^{A(0)} = 0 \tag{4.16}$$

$$\sigma_{n+1}^{(0)} = \sigma_{n+1}^{\text{trial}} = c_n \epsilon_{n+1} \tag{4.17}$$

$$\mathbf{N}_{A,n+1}^{(0)} = c_n \partial_\sigma f_{A,n+1}^{(0)} \tag{4.18}$$

$$c_{n+1}^{(0)} = c_n \tag{4.19}$$

$$k = 0 \tag{4.20}$$

Step 2. Update stress and hardening parameters:

$$\sigma_{n+1}^{(k)} = \sigma_{n+1}^{\text{trial}} - \sum_{B \in J_{\text{act}}^{(k)}} \delta\lambda^{B(k)} \mathbf{N}_{B,n+1}^{(k)} \tag{4.21}$$

$$\alpha_{A,n+1}^{(k)} = \alpha_{A,n} + \delta\lambda^{A(k)}, \ A \in J_{\text{act}}^{(k)} \tag{4.22}$$

$$\alpha_{A,n+1}^{(k)} = \alpha_{A,n}, \ A \notin J_{\text{act}}^{(k)} \tag{4.23}$$

$$q_{A,n+1}^{(k)} = -\partial_{\alpha_A} \mathcal{H}\left(\alpha_{1,n+1}^{(k)}, \alpha_{2,n+1}^{(k)}, \ldots, \alpha_{m,n+1}^{(k)}\right) \tag{4.24}$$

Step 3. Check for failure and convergence:

If $(k = 0)$ then

63

$$\phi_{A,n+1}^{(0)} = f_{A,n+1}^{(0)} + q_{A,n+1}^{(0)} - \sigma_A \tag{4.25}$$

$$J_{\text{act}}^{(0)} = \left\{ A \mid \phi_{A,n+1}^{(0)} > 0, \ A = 1, 2, \ldots, m \right\} \tag{4.26}$$

else

$$\phi_{A,n+1}^{(k)} = f_{A,n+1}^{(k)} + q_{A,n+1}^{(k)} - \sigma_A, \ A \in J_{\text{act}}^{(k)} \tag{4.27}$$

endif

If $((k = 0$ and $J_{\text{act}}^{(k)} = \emptyset)$ or $(|\phi_{A,n+1}^{(k)}| \leq$ TOL for all $A \in J_{\text{act}}^{(k)}))$ then

$$\sigma_{n+1} = \sigma_{n+1}^{(k)} \tag{4.28}$$

$$c_{n+1} = c_{n+1}^{(k)} \tag{4.29}$$

$$\alpha_{A,n+1} = \alpha_{A,n+1}^{(k)}, \ A \in J_{\text{act}}^{(k)} \tag{4.30}$$

$$\alpha_{A,n+1} = \alpha_{A,n}, \ A \notin J_{\text{act}}^{(k)} \tag{4.31}$$

return

endif

Step 4. Compute $\delta\lambda$-increments:

For $A, B \in J_{\text{act}}^{(k)}$

$$D_{n+1}^{AB\ (k)} = - \left(\partial_{\boldsymbol{\sigma}} f_{A,n+1}^{(k)} \cdot \mathbf{N}_{B,n+1}^{(k)} + \partial_{\alpha_A \alpha_B}^2 \mathcal{H}_{n+1}^{(k)} \right) \tag{4.32}$$

$$\left\{ \delta\lambda^{A(k+1)} \right\} = \left\{ \delta\lambda^{A(k)} \right\} - \left[D_{n+1}^{AB\ (k)} \right]^{-1} \left\{ \phi_{B,n+1}^{(k)} \right\} \tag{4.33}$$

$$J_{\text{temp}} = \left\{ A \in J_{\text{act}}^{(k)} \mid \delta\lambda^{A(k+1)} > 0 \right\} \tag{4.34}$$

If $(J_{\text{act}}^{(k)} \neq J_{\text{temp}})$ then

$$J_{\text{act}}^{(k)} = J_{\text{temp}} \tag{4.35}$$

For $A \notin J_{\text{act}}^{(k)}$

$$\delta \lambda^{A(k)} = 0 \tag{4.36}$$

Go to Step 2.

else

$$J_{\text{act}}^{(k+1)} = J_{\text{temp}} \tag{4.37}$$

endif

Step 5. Update return directions and moduli:

$$\mathbf{N}_{A,n+1}^{(k+1)} = \mathbf{c}_{n+1}^{(k)} \partial_{\sigma} f_{A,n+1}^{(k)}, \;\; A \in J_{\text{act}}^{(k+1)} \tag{4.38}$$

$$\mathbf{c}_{n+1}^{(k+1)} = \mathbf{c}_n - \sum_{A \in J_{\text{act}}^{(k+1)}} \delta \lambda^{A(k+1)} \frac{\mathbf{N}_{A,n+1}^{(k+1)} \otimes \mathbf{N}_{A,n+1}^{(k+1)}}{\epsilon_{n+1} \cdot \mathbf{N}_{A,n+1}^{(k+1)}} \tag{4.39}$$

Set $k = k + 1$ and go to Step 2.

Remarks

1. We note that $\phi_{A,n+1}^{(0)} > 0$ does not guarantee that surface A will ultimately be active. By construction, $J_{\text{act}}^{(k+1)} \subset J_{\text{act}}^{(k)}$.

2. The linear system of equations (4.33) reflects a Newton-like iteration to force

$$\phi_{A,n+1} = 0, \;\; A \in J_{\text{act}} \tag{4.40}$$

65

The similarity between (4.33) and (2.113) should be noted.

4.2 Rate-dependent Damage Model

The viscous regularization of the multi-surface theory follows closely the development of the single surface theory — see Section 2.5. It is given in Box 5 for completeness.

Box 5. *A multiple failure surface, small-deformation anisotropic rate-dependent damage constitutive theory.*

Constitutive equation:

$$\boldsymbol{\sigma} = \mathbf{c}\boldsymbol{\epsilon} \tag{4.41}$$

Hardening law:

$$\dot{q}_A = -\sum_{B=1}^{m} \frac{\langle \chi(\phi_B) \rangle}{\tau} \partial^2_{\alpha_A \alpha_B} \mathcal{H} \tag{4.42}$$

Damage evolution law:

$$\dot{\mathbf{c}} = -\sum_{B=1}^{m} \frac{\langle \chi(\phi_B) \rangle}{\tau} \frac{\mathbf{c}\partial_{\boldsymbol{\sigma}} f_B \otimes \mathbf{c}\partial_{\boldsymbol{\sigma}} f_B}{\partial_{\boldsymbol{\sigma}} f_B \cdot \mathbf{c}\boldsymbol{\epsilon}} \tag{4.43}$$

66

4.2.1 Algorithm for the Rate-dependent Damage Model

Numerical integration of the equations can be performed the same way as for the single surface case. The procedure is described in Algorithm 9 (cf. Algorithm 5).

Algorithm 9. *Updated explicit/implicit algorithm for the multiple failure surface, small-deformation anisotropic elastic damage constitutive theory of Box 4, or rate-dependent damage constitutive theory of Box 5.*

Step 1. Initialize:

$$\text{lvisc} = \begin{cases} \text{true,} & \text{rate-dependent damage} \quad \text{(Box 5)} \\ \text{false,} & \text{elastic damage} \quad\quad\quad \text{(Box 4)} \end{cases}$$

$$\text{lquit} = \text{false}$$

$$\Delta t_{n+1} = t_{n+1} - t_n \tag{4.44}$$

$$t_{n+1}^{(0)} = t_n \tag{4.45}$$

$$\delta \lambda^{A^{(0)}} = 0 \tag{4.46}$$

$$\sigma_{n+1}^{(0)} = \sigma_{n+1}^{\text{trial}} = c_n \epsilon_{n+1} \tag{4.47}$$

$$\mathbf{N}_{A,n+1}^{(0)} = c_n \partial_\sigma f_{A,n+1}^{(0)} \tag{4.48}$$

$$c_{n+1}^{(0)} = c_n \tag{4.49}$$

$$k = 0 \tag{4.50}$$

Step 2. Update stress and hardening parameters:

$$\sigma_{n+1}^{(k)} = \sigma_{n+1}^{\text{trial}} - \sum_{B \in J_{\text{act}}^{(k)}} \delta\lambda^{B(k)} \mathbf{N}_{B,n+1}^{(k)} \tag{4.51}$$

$$\alpha_{A,n+1}^{(k)} = \alpha_{A,n} + \delta\lambda^{A(k)}, \ A \in J_{\text{act}}^{(k)} \tag{4.52}$$

$$\alpha_{A,n+1}^{(k)} = \alpha_{A,n}, \ A \notin J_{\text{act}}^{(k)} \tag{4.53}$$

$$q_{A,n+1}^{(k)} = -\partial_{\alpha_A} \mathcal{H} \left(\alpha_{1,n+1}^{(k)}, \alpha_{2,n+1}^{(k)}, \ldots, \alpha_{m,n+1}^{(k)} \right) \tag{4.54}$$

Step 3. Check for failure and convergence:

If ($k = 0$) then

$$\phi_{A,n+1}^{(0)} = f_{A,n+1}^{(0)} + q_{A,n+1}^{(0)} - \sigma_A \tag{4.55}$$

$$J_{\text{act}}^{(0)} = \left\{ A \mid \phi_{A,n+1}^{(0)} > 0, \ A = 1, 2, \ldots, m \right\} \tag{4.56}$$

else

$$\phi_{A,n+1}^{(k)} = f_{A,n+1}^{(k)} + q_{A,n+1}^{(k)} - \sigma_A, \ A \in J_{\text{act}}^{(k)} \tag{4.57}$$

endif

If (($k = 0$ and $J_{\text{act}}^{(k)} = \emptyset$) or

(lvisc = false and $|\phi_{A,n+1}^{(k)}| \leq$ TOL for all $A \in J_{\text{act}}^{(k)}$)) then lquit = true

If (lquit = true) then

$$\sigma_{n+1} = \sigma_{n+1}^{(k)} \tag{4.58}$$

$$\mathbf{c}_{n+1} = \mathbf{c}_{n+1}^{(k)} \tag{4.59}$$

$$\alpha_{A,n+1} = \alpha_{A,n+1}^{(k)}, \ A \in J_{\text{act}}^{(k)} \tag{4.60}$$

$$\alpha_{A,n+1} = \alpha_{A,n}, \quad A \notin J_{\text{act}}^{(k)} \tag{4.61}$$

return

endif

Step 4. Compute $\delta\lambda$-increments:

For $A, B \in J_{\text{act}}^{(k)}$

$$D_{n+1}^{AB\,(k)} = - \left(\partial_{\boldsymbol{\sigma}} f_{A,n+1}^{(k)} \cdot \mathbf{N}_{B,n+1}^{(k)} + \partial_{\alpha_A \alpha_B}^2 \mathcal{H}_{n+1}^{(k)} \right) \tag{4.62}$$

If (lvisc = false) then

$$\left\{ \delta\lambda^{A(k+1)} \right\} = \left\{ \delta\lambda^{A(k)} \right\} - \left[D_{n+1}^{AB\,(k)} \right]^{-1} \left\{ \phi_{A,n+1}^{(k)} \right\}, \quad A, B \in J_{\text{act}}^{(k)} \tag{4.63}$$

else

$$\bar{t}_{n+1}^{(k)} = \frac{\tau}{S} \tag{4.64}$$

$$\Delta t_{n+1}^{(k)} = \bar{t}_{n+1}^{(k)} \left[1 - \exp\left(\frac{-\Delta t_{n+1}}{\bar{t}_{n+1}^{(k)}} \right) \right] \tag{4.65}$$

$$\delta\lambda^{A(k+1)} = \delta\lambda^{A(k)} + \Delta t_{n+1}^{(k)} \chi_{A,n+1}^{(k+1)}/\tau, \quad A \in J_{\text{act}}^{(k)} \tag{4.66}$$

endif

$$J_{\text{temp}} = \left\{ A \in J_{\text{act}}^{(k)} \mid \delta\lambda^{A(k+1)} > 0 \right\} \tag{4.67}$$

If ($J_{\text{act}}^{(k)} \neq J_{\text{temp}}$) then

$$J_{\text{act}}^{(k)} = J_{\text{temp}} \tag{4.68}$$

For $A \notin J_{\text{act}}^{(k)}$

$$\delta\lambda^{A(k)} = 0 \tag{4.69}$$

Go to Step 2.

else

    If (lvisc = true) then

$$t_{n+1}^{(k+1)} = t_{n+1}^{(k)} + \Delta t_{n+1}^{(k)} \tag{4.70}$$

    If $(t_{n+1}^{(k+1)} - t_{n+1} \geq 0)$ then

$$\Delta t_{n+1}^{(k)} = \Delta t_{n+1}^{(k)} - \left(t_{n+1}^{(k+1)} - t_{n+1} \right) \tag{4.71}$$

    lquit = true

    endif

endif

$$J_{\text{act}}^{(k+1)} = J_{\text{temp}} \tag{4.72}$$

endif

Step 5. Update return directions and moduli:

$$\mathbf{N}_{A,n+1}^{(k+1)} = \mathbf{c}_{n+1}^{(k)} \partial_{\boldsymbol{\sigma}} f_{A,n+1}^{(k)}, \ A \in J_{\text{act}}^{(k+1)} \tag{4.73}$$

$$\mathbf{c}_{n+1}^{(k+1)} = \mathbf{c}_n - \sum_{A \in J_{\text{act}}^{(k+1)}} \delta \lambda^{A(k+1)} \frac{\mathbf{N}_{A,n+1}^{(k+1)} \otimes \mathbf{N}_{A,n+1}^{(k+1)}}{\epsilon_{n+1} \cdot \mathbf{N}_{A,n+1}^{(k+1)}} \tag{4.74}$$

Set $k = k + 1$ and go to Step 2.

Remarks:

1. The parameter S in (4.64) has the same physical meaning as $-\chi_{n+1}^{\prime(k)}D\phi_{n+1}^{(k)}$ in the single surface algorithm; cf., e.g., (3.46). Because we now have a matrix D^{AB} to deal with, we need an economical way to bound its eigenvalues. This can be accomplished through Gerschgorin's circle theorem[15]. We define

$$\tilde{D}^{AB} = \chi_{A,n+1}^{\prime(k)}D_{n+1}^{AB(k)}, \quad A, B \in J_{act}^{(k)} \tag{4.75}$$

We define the radii of the Gerschgorin circles by

$$\tilde{R}^A = \sum_{\substack{B \in J_{act}^{(k)} \\ B \neq A}} |\tilde{D}^{AB}| \tag{4.76}$$

Then,

$$S = \left| \min_{A \in J_{act}^{(k)}} \left(\tilde{D}^{AA} - \tilde{R}^A \right) \right| \tag{4.77}$$

This value of S provides a lower bound for $\tilde{t}_{n+1}^{(k)}$, and thus provides a conservative estimate for stability purposes.

4.3 Plane Stress Algorithm for the Rate-independent Damage Model

Generalization of the single surface plane stress inviscid algorithm to multiple surfaces is straightforward: just as in the single surface algorithm, we introduce an extra unknown

ϵ_{33} and an extra equation,

$$\sigma_{33} = 0 \qquad (4.78)$$

Derivation of the algorithm follows along the same lines as for the single surface algorithm described in Section 3.1. It is presented here in detail for completeness.

Algorithm 10. *Updated explicit/implicit plane stress algorithm for the multiple failure surface, small-deformation anisotropic elastic damage constitutive theory of Box 4.*

Step 1. Initialize:

$$\delta \lambda^{A(0)} = 0 \qquad (4.79)$$

$$\epsilon = \epsilon_{n+1} \qquad (4.80)$$

$$\epsilon_{33}^{(0)} = -\frac{c_{n,3311}\epsilon_{11} + c_{n,3322}\epsilon_{22} + 2c_{n,3312}\epsilon_{12} + 2c_{n,3323}\epsilon_{23} + 2c_{n,3313}\epsilon_{13}}{c_{n,3333}} \qquad (4.81)$$

$$\sigma_{n+1}^{(0)} = \sigma_{n+1}^{\text{trial}} = c_n \epsilon_{n+1} \qquad (4.82)$$

$$N_{A,n+1}^{(0)} = c_n \partial_\sigma f_{A,n+1}^{(0)} \qquad (4.83)$$

$$c_{n+1}^{(0)} = c_n \qquad (4.84)$$

$$k = 0 \qquad (4.85)$$

Step 2. Update stress and hardening parameters:

$$\sigma_{n+1}^{(k)} = c_n \epsilon_{n+1}^{(k)} - \sum_{B \in J_{\text{act}}^{(k)}} \delta\lambda^{B(k)} N_{B,n+1}^{(k)} \qquad (4.86)$$

72

$$\alpha_{A,n+1}^{(k)} = \alpha_{A,n} + \delta\lambda^{A(k)}, A \in J_{\text{act}}^{(k)} \tag{4.87}$$

$$\alpha_{A,n+1}^{(k)} = \alpha_{A,n}, A \notin J_{\text{act}}^{(k)} \tag{4.88}$$

$$q_{A,n+1}^{(k)} = -\partial_{\alpha_A}\mathcal{H}\left(\alpha_{1,n+1}^{(k)}, \alpha_{2,n+1}^{(k)}, \ldots, \alpha_{m,n+1}^{(k)}\right) \tag{4.89}$$

Step 3. Check for failure and convergence:

If $(k = 0)$ then

$$\phi_{A,n+1}^{(0)} = f_{A,n+1}^{(0)} + q_{A,n+1}^{(0)} - \sigma_A \tag{4.90}$$

$$J_{\text{act}}^{(0)} = \left\{A \mid \phi_{A,n+1}^{(0)} > 0, \ A = 1, 2, \ldots, m\right\} \tag{4.91}$$

else

$$\phi_{A,n+1}^{(k)} = f_{A,n+1}^{(k)} + q_{A,n+1}^{(k)} - \sigma_A \tag{4.92}$$

endif

If $((k = 0$ and $J_{\text{act}}^{(0)} = \emptyset)$ or

$(|\phi_{A,n+1}^{(k+1)}| \leq \text{TOL}_1$ for all $A \in J_{\text{act}}^{(k)}$ and $|\sigma_{n+1,33}^{(k)}| < \text{TOL}_2))$ then

$$\boldsymbol{\sigma}_{n+1} = \boldsymbol{\sigma}_{n+1}^{(k)} \tag{4.93}$$

$$\mathbf{c}_{n+1} = \mathbf{c}_{n+1}^{(k)} \tag{4.94}$$

$$\alpha_{A,n+1} = \alpha_{A,n+1}^{(k)}, A \in J_{\text{act}}^{(k)} \tag{4.95}$$

$$\alpha_{A,n+1} = \alpha_{A,n}, A \notin J_{\text{act}}^{(k)} \tag{4.96}$$

return

endif

<u>Step 4.</u> Compute $\delta\lambda$-increments and ϵ_{33} increment:

For $A, B \in J_{\mathrm{act}}^{(k)}$

$$D_{n+1}^{AB\,(k)} = -\left(\partial_{\boldsymbol{\sigma}} f_{A,n+1}^{(k)} \cdot \mathbf{N}_{B,n+1}^{(k)} + \partial_{\alpha_A \alpha_B}^2 \mathcal{H}_{n+1}^{(k)}\right) \tag{4.97}$$

$$\left\{ \begin{array}{c} \left\{\delta\lambda^{A(k+1)}\right\} \\ \epsilon_{n+1,33}^{(k+1)} \end{array} \right\} = \left\{ \begin{array}{c} \left\{\delta\lambda^{A(k)}\right\} \\ \epsilon_{n+1,33}^{(k)} \end{array} \right\} -$$

$$\left[\begin{array}{cc} \left[D_{n+1}^{AB\,(k)}\right] & \left\{\mathbf{c}_n \partial f_A\right\} \\ -\left\{N_{B,n+1,33}^{(k)}\right\}^T & c_{n,3333} \end{array} \right]^{-1} \left\{ \begin{array}{c} \left\{\phi_{A,n+1}^{(k)}\right\} \\ \sigma_{n+1,33}^{(k)} \end{array} \right\}, \ A, B \in J_{\mathrm{act}}^{(k)} \tag{4.98}$$

$$J_{\mathrm{temp}} = \left\{ A \in J_{\mathrm{act}}^{(k)} \mid \delta\lambda^{A(k+1)} > 0 \right\} \tag{4.99}$$

If $(J_{\mathrm{act}}^{(k)} \neq J_{\mathrm{temp}})$ then

$$J_{\mathrm{act}}^{(k)} = J_{\mathrm{temp}} \tag{4.100}$$

For $A \notin J_{\mathrm{act}}^{(k)}$

$$\delta\lambda^{A(k)} = 0 \tag{4.101}$$

Go to Step 2.

else

$$J_{\mathrm{act}}^{(k+1)} = J_{\mathrm{temp}} \tag{4.102}$$

endif

Step 5. Update return direction and moduli:

$$\mathbf{N}^{(k+1)}_{A,n+1} = \mathbf{c}^{(k)}_{n+1} \partial_{\boldsymbol{\sigma}} f^{(k)}_{A,n+1}; \quad A \in J^{(k)}_{\text{act}} \tag{4.103}$$

$$\mathbf{c}^{(k+1)}_{n+1} = \mathbf{c}_n - \sum_{A \in J^{(k+1)}_{\text{act}}} \delta\lambda^{A(k+1)} \frac{\mathbf{N}^{(k+1)}_{A,n+1} \otimes \mathbf{N}^{(k+1)}_{A,n+1}}{\boldsymbol{\epsilon}^{(k+1)}_{n+1} \cdot \mathbf{N}^{(k+1)}_{A,n+1}} \tag{4.104}$$

Set $k = k + 1$ and go to Step 2.

4.4 Plane Stress Algorithm for the Rate-dependent Damage Model

The integration algorithm for the plane stress, multiple surface theory with regularization follows, once again, along the lines of the single surface theory. At the end of the inviscid calculation the viscoplastic regularization is done, the 33-strain is updated to account for the ZNS constraint, and the final stress is computed.

Algorithm 11. *Updated explicit/implicit plane stress algorithm for the multiple failure surface, small-deformation anisotropic elastic damage constitutive theory of Box 4, or rate-dependent damage constitutive theory of Box 5.*

Step 1. Initialize:

$$\text{lvisc} = \begin{cases} \text{true,} & \text{rate-dependent damage} & \text{(Box 5)} \\ \text{false,} & \text{elastic damage} & \text{(Box 4)} \end{cases}$$

$$\text{lquit} = \text{false}$$

$$\Delta t_{n+1} = t_{n+1} - t_n \tag{4.105}$$

$$t_{n+1}^{(0)} = t_n \tag{4.106}$$

$$\delta \lambda^{A(0)} = 0 \tag{4.107}$$

$$\epsilon = \epsilon_{n+1} \tag{4.108}$$

$$\epsilon_{33}^{(0)} = -\frac{c_{n,3311}\epsilon_{11} + c_{n,3322}\epsilon_{22} + 2c_{n,3312}\epsilon_{12} + 2c_{n,3323}\epsilon_{23} + 2c_{n,3313}\epsilon_{13}}{c_{n,3333}} \tag{4.109}$$

$$\sigma_{n+1}^{(0)} = \sigma_{n+1}^{\text{trial}} = \mathbf{c}_n \epsilon_{n+1} \tag{4.110}$$

$$\mathbf{N}_{A,n+1}^{(0)} = \mathbf{c}_n \partial_\sigma f_{A,n+1}^{(0)} \tag{4.111}$$

$$\mathbf{c}_{n+1}^{(0)} = \mathbf{c}_n \tag{4.112}$$

$$k = 0 \tag{4.113}$$

76

Step 2. Update stress and hardening parameters:

$$\sigma_{n+1}^{(k)} = c_n \epsilon_{n+1}^{(k)} - \sum_{B \in J_{\text{act}}^{(k)}} \delta\lambda^{B(k)} \mathbf{N}_{B,n+1}^{(k)} \tag{4.114}$$

$$\alpha_{A,n+1}^{(k)} = \alpha_{A,n} + \delta\lambda^{A(k)}, A \in J_{\text{act}}^{(k)} \tag{4.115}$$

$$\alpha_{A,n+1}^{(k)} = \alpha_{A,n}, A \notin J_{\text{act}}^{(k)} \tag{4.116}$$

$$q_{A,n+1}^{(k)} = -\partial_{\alpha_A} \mathcal{H}\left(\alpha_{1,n+1}^{(k)}, \alpha_{2,n+1}^{(k)}, \ldots, \alpha_{m,n+1}^{(k)}\right) \tag{4.117}$$

Step 3. Check for failure and convergence:

If ($k = 0$) then

$$\phi_{A,n+1}^{(0)} = f_{A,n+1}^{(0)} + q_{A,n+1}^{(0)} - \sigma_A \tag{4.118}$$

$$J_{\text{act}}^{(0)} = \left\{ A \mid \phi_{A,n+1}^{(0)} > 0, \ A = 1, 2, \ldots, m \right\} \tag{4.119}$$

else

$$\phi_{A,n+1}^{(k)} = f_{A,n+1}^{(k)} + q_{A,n+1}^{(k)} - \sigma_A, \ A \in J_{\text{act}}^{(k)} \tag{4.120}$$

endif

If (($k = 0$ and $J_{\text{act}}^{(0)} = \emptyset$) or

(lvisc = false and $|\phi_{A,n+1}^{(k)}| \leq \text{TOL}_1$ for all $A \in J_{\text{act}}^{(k)}$

and $|\sigma_{n+1,33}^{(k)}| < \text{TOL}_2$)) then lquit = true

If (lquit = true) then

$$\sigma_{n+1} = \sigma_{n+1}^{(k)} \tag{4.121}$$

$$c_{n+1} = c_{n+1}^{(k)} \tag{4.122}$$

$$\alpha_{A,n+1} = \alpha_{A,n+1}^{(k)}, \ A \in J_{\text{act}}^{(k)} \tag{4.123}$$

$$\alpha_{A,n+1} = \alpha_{A,n}, \ A \notin J_{\text{act}}^{(k)} \tag{4.124}$$

return

endif

Step 4. Compute $\delta\lambda$-increments and ϵ_{33} increment:

For $A, B \in J_{\text{act}}^{(k)}$

$$D_{n+1}^{AB\,(k)} = -\left(\partial_{\boldsymbol{\sigma}} f_{A,n+1}^{(k)} \cdot \mathbf{N}_{B,n+1}^{(k)} + \partial^2_{\alpha_A \alpha_B} \mathcal{H}_{n+1}^{(k)}\right) \tag{4.125}$$

If (lvisc = false) then

$$\left\{ \begin{array}{c} \left\{\delta\lambda^{A(k+1)}\right\} \\ \epsilon_{n+1,33}^{(k+1)} \end{array} \right\} = \left\{ \begin{array}{c} \left\{\delta\lambda^{A(k)}\right\} \\ \epsilon_{n+1,33}^{(k)} \end{array} \right\} -$$
$$\left[\begin{array}{cc} \left[D_{n+1}^{AB\,(k)}\right] & \left\{\mathbf{c}_n \partial f_A\right\} \\ -\left\{N_{B,n+1,33}^{(k)}\right\}^T & c_{n,3333} \end{array} \right]^{-1} \left\{ \begin{array}{c} \left\{\phi_{A,n+1}^{(k)}\right\} \\ \sigma_{n+1,33}^{(k)} \end{array} \right\}, \ A, B \in J_{\text{act}}^{(k)} \tag{4.126}$$

else

$$\bar{t}_{n+1}^{(k)} = \frac{\tau}{S} \tag{4.127}$$

$$\Delta t_{n+1}^{(k)} = \bar{t}_{n+1}^{(k)} \left[1 - \exp\left(\frac{-\Delta t_{n+1}}{\bar{t}_{n+1}^{(k)}}\right)\right] \tag{4.128}$$

$$\delta\lambda^{A(k+1)} = \delta\lambda^{A(k)} + \Delta t_{n+1}^{(k)} \chi_{A,n+1}^{(k)}/\tau, \ A \in J_{\text{act}}^{(k)} \tag{4.129}$$

$$\epsilon_{n+1,33}^{(k+1)} = -\frac{c_{n,3311}\epsilon_{11} + c_{n,3322}\epsilon_{22} + 2c_{n,3312}\epsilon_{12} + 2c_{n,3323}\epsilon_{23} + 2c_{n,3313}\epsilon_{13}}{c_{n,3333}} +$$
$$\sum_{A \in J_{\text{act}}^{(k)}} \frac{\delta\lambda^{A(k+1)} N_{n+1,33}^{(k)}}{c_{n,3333}} \tag{4.130}$$

endif

$$J_{\text{temp}} = \left\{ A \in J_{\text{act}}^{(k)} \mid \delta\lambda^{A(k+1)} > 0 \right\} \tag{4.131}$$

If ($J_{\text{act}}^{(k)} \neq J_{\text{temp}}$) then

$$J_{\text{act}}^{(k)} = J_{\text{temp}} \qquad (4.132)$$

For $A \notin J_{\text{act}}^{(k)}$

$$\delta \lambda^{A(k)} = 0 \qquad (4.133)$$

Go to Step 2.

else

If (lvisc = true) then

$$t_{n+1}^{(k+1)} = t_{n+1}^{(k)} + \Delta t_{n+1}^{(k)} \qquad (4.134)$$

If ($t_{n+1}^{(k+1)} - t_{n+1} \geq 0$) then

$$\Delta t_{n+1}^{(k)} = \Delta t_{n+1}^{(k)} - \left(t_{n+1}^{(k+1)} - t_{n+1} \right) \qquad (4.135)$$

lquit = true

endif

endif

$$J_{\text{act}}^{(k+1)} = J_{\text{temp}} \qquad (4.136)$$

endif

Step 5. Update return direction and moduli:

$$\mathbf{N}_{A,n+1}^{(k+1)} = \mathbf{c}_{n+1}^{(k)} \partial_{\boldsymbol{\sigma}} f_{A,n+1}^{(k)}, \ A \in J_{\text{act}}^{(k)} \qquad (4.137)$$

$$\mathbf{c}_{n+1}^{(k+1)} = \mathbf{c}_n - \sum_{A \in J_{\text{act}}^{(k+1)}} \delta \lambda^{A(k+1)} \frac{\mathbf{N}_{A,n+1}^{(k+1)} \otimes \mathbf{N}_{A,n+1}^{(k+1)}}{\epsilon_{n+1}^{(k+1)} \cdot \mathbf{N}_{A,n+1}^{(k+1)}} \qquad (4.138)$$

79

Set $k = k + 1$ and go to Step 2.

Chapter 5

Conclusions

In this report we have considered a variety of three-dimensional and plane stress constitutive models and algorithms for reinforced concrete plate and shell structures. Anisotropic damage mechanisms have been accounted for to provide a setting for incorporating various failure phenomena within a homogenized, or distributed, constitutive representation. Rate-dependent effects have been introduced by way of a viscous regularization technique. This feature is useful for faithfully modeling high rates of loading, and also provides a constitutive framework which avoids certain numerical pitfalls associated with strain-softening behavior. Multiple failure surface theories have also been investigated. These are useful for the development of damage theories based upon often-used, multiple surface theories, such as the cap model, and related potentially useful theories employed in the modeling of fiber-reinforced composites.

Bibliography

[1] D. P. Bertsekas. *Constrained Optimization and Lagrange Multiplier Methods*. Academic Press, 1982.

[2] M. Cervera, E. Hinton, and N. Bicanic. Non-linear Transient Dynamic Analysis of Three-dimensional Reinforced Concrete Structures. *Numerical Methods for Transient and Coupled Problems*. Wiley, 1987.

[3] M. Cervera, E. Hinton, and O. Hassan. Nonlinear Analysis of Reinforced Concrete Plate and Shell Structures Using 20-Noded Isoparametric Brick Elements. *Computers and Structures*. Wiley, 1987.

[4] Z. Hashin. Failure criteria for uni-directional fiber composites. *Journal of Applied Mechanics*, 47, 1980.

[5] L. Herrmann. Work in progress. U. C. Davis.

[6] R. Hill. *The Mathematical Theory of Plasticity*. Oxford University Press, 1950.

[7] T. J. R. Hughes and W. K. Liu. *Nonlinear Finite Element Analysis of Shells: Part I. Three-dimensional Shells.* Computer Methods in Applied Mechanics and Engineering. 27, 1981.

[8] T. J. R. Hughes. Numerical Implementation of Constitutive Models: Rate-independent Deviatoric Plasticity. *Theoretical Foundations for Large-scale Computations for Nonlinear Material Behavior.* Martinus-Nijhoff Publishers, 1984.

[9] T. J. R. Hughes. *An Assessment of Modelling Techniques for the Finite Finite Element Analysis of Reinforced Concrete Plate and Shell Structures.* Technical Report CR 88.008, Naval Civil Engineering Laboratory, Port Hueneme, 1986.

[10] T. J. R. Hughes. *The Finite Element Method.* Prentice Hall, 1987.

[11] T. J. R. Hughes. *Efficient and Simple Algorithms for the Integration of General Classes of Inelastic Constitutive Equations Including Damage and Rate Effects: Application to the Cap Model for Soils and Concrete.* Technical Report CR 87.004, Naval Civil Engineering Laboratory, Port Hueneme, 1987.

[12] R. M. Jones. *Mechanics of Composite Materials.* Hemisphere Publishing Corporation, 1975.

[13] H. Kupfer, H. K. Hilsdorf, and H. Rusch. Behavior of concrete under biaxial stresses. *Journal of the American Concrete Institute,* 66(8), 1969.

[14] D. Luenberger. *Linear and Nonlinear Programming.* Addison-Wesley, 1984.

[15] B. Noble. *Applied Linear Algebra.* Prentice Hall, 1969.

[16] P. Perzyna. Fundamental Problems in Viscoplasticity. *Advances in Applied Mechanics,* 29, 1966.

[17] J. C. Simo and T. J. R. Hughes. General return mapping algorithms for rate-independent plasticity. In C.S. Desai, E. Krempl, P.D. Kiousis, and T. Kundu, editors, *Constitutive Laws for Engineering Materials — Theory and Application.* Elsevier, January 1987.

[18] J. C. Simo and T. J. R. Hughes. *Elastoplasticity and Viscoplasticity — Computational Aspects.* Technical Report, Stanford University, 1988.

[19] J. C. Simo, J. E. Kennedy, and S. Govindjee. Rate-independent plasticity with non-smooth multi-yield surfaces: loading/unloading conditions and numerical algorithms. *International Journal for Numerical Methods in Engineering,* 1988.

[20] J. C. Simo. *Some Aspects of Continuum Damage Mechanics and Strain Softening.* Technical Report, Stanford University, 1989.

[21] G. M. Stanley. *Continuum-Based Shell Elements.* PhD thesis, Stanford University, August 1985.

[22] G. M. Stanley and T. J. R. Hughes. *Finite Element Procedures Applicaole to Nonlinear Analysis of Reinforced Concrete Shell Structures.* Technical Report CR 84.033. Naval Civil Engineering Laboratory, Port Hueneme. 1984.

[23] K. Valanis. On the Uniqueness of Solution of the Initial Value Problem in Softening Materials. *Journal of Applied Mechanics,* 52, 1985.

NCEL DOCUMENT EVALUATION

You are number one with us; how do we rate with you?

We at NCEL want to provide you our customer the best possible reports but we need your help. Therefore, I ask you to please take the time from your busy schedule to fill out this questionnaire. Your response will assist us in providing the best reports possible for our users. I wish to thank you in advance for your assistance. I assure you that the information you provide will help us to be more responsive to your future needs.

R. N. Storer

R. N. STORER, Ph.D, P.E.
Technical Director

DOCUMENT NO. _____ TITLE OF DOCUMENT: _____

_____

Date: _____ Respondent Organization : _____

Name: _____ Activity Code: _____
Phone: _____ Grade/Rank: _____

Category (*please check*):

Sponsor _____ User _____ Proponent _____ Other (*Specify*) _____

Please answer on your behalf only; not on your organization's. Please check (*use an X*) only the block that most closely describes your attitude or feeling toward that statement:

SA Strongly Agree **A** Agree **O** Neutral **D** Disagree **SD** Strongly Disagree

---

		SA A N D SD
1.	The technical quality of the report is comparable to most of my other sources of technical information.	( ) ( ) ( ) ( ) ( )
2.	The report will make significant improvements in the cost and or performance of my operation.	( ) ( ) ( ) ( ) ( )
3.	The report acknowledges related work accomplished by others.	( ) ( ) ( ) ( ) ( )
4.	The report is well formatted.	( ) ( ) ( ) ( ) ( )
5.	The report is clearly written.	( ) ( ) ( ) ( ) ( )

		SA A N D SD
6.	The conclusions and recommendations are clear and directly supported by the contents of the report.	( ) ( ) ( ) ( ) ( )
7.	The graphics, tables, and photographs are well done.	( ) ( ) ( ) ( ) ( )

Do you wish to continue getting NCEL reports?	☐ YES	☐ NO

Please add any comments (e.g., in what ways can we improve the quality of our reports?) on the back of this form.

Comments:

Please fold on line and staple

- -

Code L03B

NAVAL CIVIL ENGINEERING LABORATORY

PORT HUENEME, CA 93043-5003